

A FREE BOUNDARY MODEL FOR TRANSPORT INDUCED NEURITE GROWTH

GRETA MARINO, JAN-FREDERIK PIETSCHMANN, AND MAX WINKLER

ABSTRACT. We introduce a free boundary model to example the effect of vesicle transport onto neurite growth. It consists of systems of drift-diffusion equations describing the evolution of the density of antero- and retrograde vesicles in each neurite coupled to reservoirs located at the soma and the growth cones of the neurites, respectively. The model allows for a change of neurite length depending on the vesicle concentration in the growth cones. After establishing existence and uniqueness for the time-dependent problem, we briefly comment on possible types of stationary solutions. Finally, we provide numerical studies on biologically relevant scales using a finite volume scheme. We illustrate the capability of the model to reproduce cycles of extension and retraction.

1. INTRODUCTION

Mature neurons are highly polarized cells featuring functionally distinct compartments, the axons and the dendrites. This polarity is established during their development. Initially, newborn neurons feature several undifferentiated extensions of similar length (neurites) that are highly dynamic [7, 12]. Eventually, one of these neurites is selected to become the axon.

The actual growth or shrinkage of neurites is due to the insertion or retraction of vesicles (i.e., circular structures composed of lipid membranes) at the outer tips of the neurites (growth cones). The vesicles themselves are produced in the cell body (soma) and then form complexes with motor proteins that allow for active transport along microtubules. The direction of transport is determined by the type of motor protein: kinesin results in anterograde transport (into the growth cones) while dynein motors move vesicles retrogradely to the soma. Both kinesins and dyneins are present on vesicles during their transport along microtubules, but only one of them is usually active at any given time [10, 22], see Figure 1 for a sketch. The actual increase of the surface area of the plasma membrane is then due to the insertion of vesicles into the growth cone (exocytosis). Retraction, on the other hand, is accompanied by the removal of membrane material from the growth cone through endocytosis [19, 18, 20].

While there are different models for the underlying biochemical processes of selecting the neurite which eventually becomes the axon (see also [17] for a recent review), mathematical models examining the role of vesicle transport in this process are relatively scarce. One exception are the works [4, 3] which, however,

2020 *Mathematics Subject Classification.* 92-08, 92C20, 35R35, 35K45, 35A05.

Key words and phrases. neurite growth, vesicle transport, free boundary problems, finite volumes, partial differential equations.

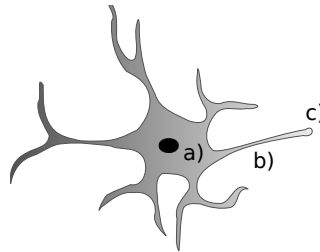


FIGURE 1. Sketch of a developing neuron. Here a) represents the cell nucleus/soma where vesicles are produced, b) a neurite and c) a growth cone, i.e., the location where vesicles are inserted/removed into the cell membrane.

focus on transport in a grown axon. In particular in [3], a limited transport capacity inside the neurites is taken into account by size exclusion effects and antero- and retrogradely moving particles are modelled separately. In [13] a similar approach is taken, yet on a microscopic particle level. Furthermore, [13] extends the model by coupling two copies of it to pools representing the amount of vesicles present at the soma and growth cones, respectively.

The aim of this paper is to introduce a macroscopic model in the spirit of both [13, 3], yet additionally allowing the length of the respective neurites to change. Different to [3] (see also [6]), our model will have linear diffusion and non-linear transport terms. Such a model can also be justified as limit of a discrete lattice model, see [14, 5]. We are able to show that the solution stays within a given interval (usually taken to be $[0, 1]$) so that the size exclusion property is preserved. Then, these equations which model transport inside the neurons are, as in [13], coupled to ordinary differential equations for the evolution of the vesicle concentration at soma and tip, respectively. One of the main novelties is then to add a mechanism which allows for growth or shrinkage of the neurites depending on how many vesicles are present in the growth cones.

1.1. Contribution and outline. We make the following contributions

- Based on [13, 3], we introduce a macroscopic model for vesicle transport in developing neuron cells that includes multiple neurites, coupled with ODEs for the vesicle concentration in soma and growth cones.
- We add a mechanism that allows for a change of neurite length depending on the respective vesicle concentration, which renders the model a free boundary problem.
- We rigorously prove existence and uniqueness of solutions, including box constraints corresponding to size exclusion effects due to the finite volume of vesicles.
- We provide a finite volume discretization that preserves the box constraints.
- Perform a scaling of the model to biological reasonable regimes and then give some numerical experiments illustrating different behaviour of the model, in particular cycles of expansion and retraction as observed in experiments.

The paper is organised as follows: In Section 2 we present our model in detail. Section 3 contains some preliminaries and is then devoted to weak solutions, while Section 4 contains a brief discussion on (constant) stationary solutions. Section 5 provides a finite volume scheme, a non-dimensionalization together with the introduction of biologically relevant scales. Section 6 is devoted to the numerical studies. Finally, Section 7 provides a brief conclusion and outlook.

2. MATHEMATICAL MODEL

In this section we present a mathematical model for the growth process based on the principles stated in the introduction. For the reader's convenience, we will focus on the case of a two neurites connected to the soma, pointing out that the generalization to multiple neurites is straightforward. For $j = 1, 2$, the unknowns of our model read as follows:

- $L_j(t)$ denotes the length of the respective neurite at time t ;
- $f_{+,j}(t, x)$ and $f_{-,j}(t, x)$ denote the density of motor-protein complexes in neurite j that moves towards the growth cone (anterograde direction) and towards the soma (retrograde direction), respectively;
- $\Lambda_{\text{som}}(t)$ is the amount of vesicles present in the soma at time t ;
- $\Lambda_j(t)$ is the amount of vesicles present in the tip of each neurite at time t .

The complete model consists of equations governing the dynamics inside each neurite, coupled with ODEs at the soma and growth cones, respectively, as well as with equations accounting for the change of the neurites lengths, see Figure 2 for an illustration of the couplings. We will discuss each component separately.

1. *Dynamics within the neurites.* Let $v_0 > 0$ be the velocity of vesicles as they move along neurites and let $\rho_j = \rho_j(t, x) := f_{+,j} + f_{-,j}$ be the total vesicle density, $j = 1, 2$. We define the fluxes of antero- and retrogradely moving vesicle-motor complexes as

$$J_{+,j} := v_0 f_{+,j}(1 - \rho_j) - D_T \partial_x f_{+,j}, \quad J_{-,j} := -v_0 f_{-,j}(1 - \rho_j) - D_T \partial_x f_{-,j}, \quad (2.1)$$

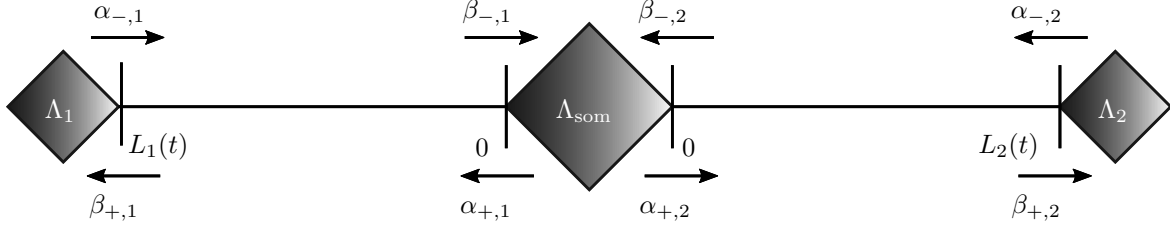


FIGURE 2. Sketch of the model neuron: it consists of two neurites modelled by two intervals $(0, L_1(t))$ and $(0, L_2(t))$. The squares correspond to pools where vesicles can be stored. More precisely, the pool in the middle corresponds to the soma while the others stand for the corresponding growth cones. The interaction between neurites and pools is realised via boundary fluxes and the parameters governing their respective strength are displayed along with arrows of the transport direction. For an easy visualisation, $(0, L_1(t))$ is illustrated as a mirrored copy of $(0, L_2(t))$.

respectively. Assume additionally that the complexes can (randomly, possibly via dissociation) change their direction with a given rate $\lambda \geq 0$. We obtain the following drift-diffusion-reaction equations, a copy of which holds true in each neurite separately,

$$\begin{aligned} \partial_t f_{+,j} &= -\partial_x J_{+,j} + \lambda(f_{-,j} - f_{+,j}), \\ \partial_t f_{-,j} &= -\partial_x J_{-,j} + \lambda(f_{+,j} - f_{-,j}), \end{aligned} \quad \text{in } (0, T) \times (0, L_j(t)), \quad (2.2)$$

where $L_j(t)$ is the current length of the domain and $T > 0$ is a fixed final time.

2. *Coupling to soma and pools.* We assume that all neurites are connected to the soma at the point $x = 0$. There, we have the following effects:

- Retrograde vesicles leave the neurite and enter the soma with rate $\beta_{-,j}(\Lambda_{\text{som}})f_{-,j}$.
- Anterograde vesicles can leave the soma and enter the lattice if there is enough space, i.e., if $\rho_j < 1$. In this case, they enter with a given rate $\alpha_{+,j}(\Lambda_{\text{som}})g_{+,j}(f_{+,j}, f_{-,j})$.

At the point $x = L_j(t)$ the neurite is connected to its respective pool and we have:

- Anterograde vesicles leave the lattice and enter the pool with rate $\beta_{+,j}(\Lambda_j)f_{+,j}$.
- Retrograde particles move from the pool into the neurite, once again only if space in the domain is available, with rate $\alpha_{-,j}(\Lambda_j)g_{-,j}(f_{+,j}, f_{-,j})$.

Figure 2 provides a sketch of this situation. This behaviour is implemented by imposing the following flux boundary conditions (for each neurite):

$$\begin{aligned} J_{+,j}(t, 0) &= \alpha_{+,j}(\Lambda_{\text{som}}(t))g_{+,j}(\mathbf{f}_j(t, 0)), \\ -J_{-,j}(t, 0) &= \beta_{-,j}(\Lambda_{\text{som}}(t))f_{-,j}(t, 0), \\ J_{+,j}(t, L_j(t)) &= \beta_{+,j}(\Lambda_j(t))f_{+,j}(t, L_j(t)), \\ -J_{-,j}(t, L_j(t)) &= \alpha_{-,j}(\Lambda_j(t))g_{-,j}(\mathbf{f}_{+,j}(t, L(t))), \end{aligned} \quad j = 1, 2, \quad (2.3)$$

for suitable functions $\alpha_{i,j}$, $\beta_{i,j}$, and $g_{i,j}$ whose properties will be specified later, and with the shortened notation $\mathbf{f}_j(\cdot, \cdot) := (f_{+,j}(\cdot, \cdot), f_{-,j}(\cdot, \cdot))$, $j = 1, 2$.

3. *Dynamics of the free boundary.* We assume that the length of each neurite L_j satisfies the following ordinary differential equation

$$L'_j(t) = h_j(\Lambda_j(t), L_j(t)), \quad (2.4)$$

where h_j , $j = 1, 2$, are smooth functions to be specified. We think of h_j as functions that change sign at a critical concentration of Λ_j (i.e., switch between growth or shrinkage), which may depend on the current length of the neurite itself (e.g. in order to stop shrinkage at a minimal length).

4. *Dynamics in soma and growth cones.* Finally, we describe the change of number of vesicles in the soma and the respective neurite growth cones, due to vesicles entering and leaving the pools. In addition, a

production term is added at the soma, while for the growth cones we add terms that model the consumption or production of vesicles due to growth or shrinkage of the neurite, respectively. We obtain

$$\begin{aligned}
\Lambda'_{\text{som}}(t) &= \sum_{j=1,2} (\beta_{-,j}(\Lambda_{\text{som}}(t)) f_{-,j}(t, 0) - \alpha_{+,j}(\Lambda_{\text{som}}(t)) g_{+,j}(\mathbf{f}_j(t, 0))) + \gamma(t), \\
\Lambda'_1(t) &= \beta_{+,1}(\Lambda_1(t)) f_{+,1}(t, L_1(t)) - \alpha_{-,1}(\Lambda_1(t)) g_{-,1}(\mathbf{f}_1(t, L_1(t))) \\
&\quad - c_1 h_1(\Lambda_1(t), L_1(t)), \\
\Lambda'_2(t) &= \beta_{+,2}(\Lambda_2(t)) f_{+,2}(t, L_2(t)) - \alpha_{-,2}(\Lambda_2(t)) g_{-,2}(\mathbf{f}_2(t, L_2(t))) \\
&\quad - c_2 h_2(\Lambda_2(t), L_2(t)),
\end{aligned} \tag{2.5}$$

where $c_1, c_2 > 0$ are given parameters.

Remark 2.1. Note that except for the growth term $\gamma(t)$, the total mass is preserved. We have

$$\sum_{j=1,2} \left(\int_0^{L_j(t)} \rho_j(t, x) dx + \Lambda_j(t) \right) + \Lambda_{\text{som}}(t) = m_0 + \int_0^t \gamma(s) ds,$$

where, for given initial conditions $\rho_j^0 = f_{+,j}^0 + f_{-,j}^0$, Λ_j^0 , Λ_{som}^0 , L_j^0 , we define the total initial mass as

$$m_0 := \sum_{j=1,2} \left(\int_0^{L_j^0} \rho_j^0(x) dx + \Lambda_j^0 \right) + \Lambda_{\text{som}}^0.$$

3. EXISTENCE OF WEAK SOLUTIONS

The aim of this section is to provide existence of a unique weak solutions to model (2.1)–(2.5). Let us first give some preliminaries.

3.1. Preliminaries. Let $L > 0$ and let $1 \leq p < \infty$. We denote by $L^p(0, L)$ and $W^{1,p}(0, L)$ the usual Lebesgue and Sobolev spaces. For $p = 2$ we write $H^1(0, L)$ instead of $W^{1,2}(0, L)$. Furthermore, $H^1(0, L)'$ is the dual space of $H^1(0, L)$.

It is well known (see, e.g. [1]) that there exists a unique linear, continuous map $\Gamma: W^{1,p}(0, L) \rightarrow \mathbb{R}$ known as the trace map such that $\Gamma(u) = u(0)$ for all $u \in W^{1,p}(0, L) \cap C([0, L])$. In addition, let us recall the following trace estimate [2, Theorem 1.6.6]

$$|u(0)| \leq C_e \|u\|_{L^2(0,L)}^{1/2} \|u\|_{H^1(0,L)}^{1/2}. \tag{3.1}$$

Let $T > 0$ and let $(B, \|\cdot\|_B)$ be a Banach space. For every $1 \leq r < \infty$ we denote by $L^r((0, T); B)$ the Bochner space of all measurable functions $u: [0, T] \rightarrow B$ such that $\|u\|_{L^r((0,T);B)}^r := \int_0^T \|u(t)\|_B^r dt < \infty$. For $r = \infty$ the norm of the corresponding space $L^\infty((0, T); B)$ is given by $\|u\|_{L^\infty((0,T);B)} := \text{ess sup}_{0 \leq t \leq T} \|u(t)\|_B$. Finally, $C([0, T]; B)$ contains all continuous functions $u: [0, T] \rightarrow B$ such that

$$\|u\|_{C([0,T];B)} := \max_{0 \leq t \leq T} \|u(t)\|_B < \infty.$$

We refer to [11] as a reference for the Bochner spaces. For every $a \in \mathbb{R}$ we set $a^\pm := \max\{\pm a, 0\}$ and for $u \in W^{1,p}(0, L)$ we define $u^\pm(\cdot) := u(\cdot)^\pm$ and will use the fact that $u^\pm \in W^{1,p}$.

3.2. Notion of weak solution and existence result. We now define the notion of weak solution to our problem. Whenever not differently specified, we assume $i \in \{+, -\}$ as well as $j \in \{1, 2\}$, $k \in \{1, 2, \text{som}\}$, while $C > 0$ denotes a constant that may change from line to line but always depends only on the data.

Definition 3.1. We say that $(\mathbf{f}_1, \mathbf{f}_2, \Lambda_{\text{som}}, \Lambda_1, \Lambda_2, L_1, L_2)$ is a weak solution to (2.1)–(2.5) if

- (a) $0 \leq f_{i,j} \leq 1$ as well as $\rho_j := f_{+,j} + f_{-,j} \leq 1$ for a.e. $x \in (0, L_j(t))$, $t \in (0, T)$;
- (b) $f_{i,j} \in L^2((0, T); H^1(0, L_j(t)))$ with $\partial_t f_{i,j} \in L^2((0, T); H^1(0, L_j(t))')$;

(c) \mathbf{f}_j solves (2.1)–(2.3) in the following weak sense

$$\begin{aligned} \int_0^{L_j(t)} \partial_t f_{+,j} \varphi_+ dx &= \int_0^{L_j(t)} (v_0 f_{+,j} (1 - \rho_j) - D_T \partial_x f_{+,j}) \partial_x \varphi_+ + \lambda (f_{-,j} - f_{+,j}) \varphi_+ dx \\ &\quad - \beta_{+,j}(\Lambda_j) f_{+,j}(t, L_j(t)) \varphi_+(L_j(t)) + \alpha_{+,j}(\Lambda_{\text{som}}) g_{+,j}(\mathbf{f}_j(t, 0)) \varphi_+(0), \\ \int_0^{L_j(t)} \partial_t f_{-,j} \varphi_- dx &= \int_0^{L_j(t)} -(v_0 f_{-,j} (1 - \rho_j) + D_T \partial_x f_{-,j}) \partial_x \varphi_- + \lambda (f_{+,j} - f_{-,j}) \varphi_- dx \\ &\quad + \alpha_{-,j}(\Lambda_j) g_{-,j}(\mathbf{f}_j(t, L_j(t))) \varphi_-(L_j(t)) - \beta_{-,j} f_{-,j}(t, 0) \varphi_-(0), \end{aligned}$$

for every $\varphi_+, \varphi_- \in H^1(0, L_j(t))$ and almost everywhere in $(0, T)$.

(d) $L_j(0) = L_j^0$, $\Lambda_k(0) = \Lambda_k^0$, and $\mathbf{f}_j(0, x) = \mathbf{f}_j^0(x)$ a.e. in $(0, L_j^0)$, for suitable L_j^0, Λ_k^0 , and \mathbf{f}_j^0 ;

(e) $\Lambda_k \in C^1([0, T])$ solves (2.5);

(f) $L_j \in C^1([0, T])$ solves (2.4).

We next state the assumptions on the data. It holds:

(H₀) $\Lambda_k^0 > 0$ and $L_j^0 \geq \ell_j$, where $\ell_j > 0$ is given.

(H₁) For $f_{+,j}^0, f_{-,j}^0 \in L^2(0, L_j^0)$ it holds $f_{+,j}^0, f_{-,j}^0 \geq 0$ and $0 \leq \rho_j^0 \leq 1$ a.e. in $(0, L_j^0)$, where $\rho_j^0 := f_{+,j}^0 + f_{-,j}^0$.

(H₂) The nonlinearities $g_{i,j}: \mathbb{R}^2 \rightarrow \mathbb{R}_+$, are Lipschitz continuous and such that $g_{i,j}(s, t) = 0$ whenever $s+t = 1$ as well as $g_{-,j}(s, 0) = g_{+,j}(0, s) = 0$ for all $0 \leq s \leq 1$.

(H₃) The functions $h_j: \mathbb{R}_+ \times [\ell_j, +\infty) \rightarrow \mathbb{R}$ are such that

(i) h_j are Lipschitz continuous;

(ii) $h_j(s, \cdot)$ is increasing for all $s \in \mathbb{R}$ and there exists (s^*, t^*) such that $h_j(s^*, t^*) = 0$.

(iii) $h_j(s, \ell_j) > 0$ for every $s \geq 0$.

(H₄) The functions $\alpha_{i,j}: \mathbb{R}_+ \rightarrow \mathbb{R}_+$ are increasing and Lipschitz continuous. Moreover, $\alpha_{-,j}(t) \geq 0$ for all $t > 0$ and $\alpha_{-,j}(0) = 0$.

(H₅) The functions $\beta_{i,j}: \mathbb{R}_+ \rightarrow \mathbb{R}_+$ are nonnegative and Lipschitz continuous. Moreover, there exists $\Lambda_{j,\max} > 0$ such that $\beta_{+,j}(\Lambda_{j,\max}) = 0$.

(H₆) The parameters satisfy $v_0, D_T, c_j > 0$ and $\lambda \geq 0$.

(H₇) The function $\gamma: \mathbb{R}_+ \rightarrow \mathbb{R}_+$ is such that $\lim_{t \rightarrow \infty} \gamma(t) = 0$.

Then we can state our existence result for system (2.1)–(2.5).

Theorem 3.2. *Let the assumptions (H₀)–(H₆) hold. Then, for every $T > 0$ there exists a unique weak solution $(\mathbf{f}_1, \mathbf{f}_2, \Lambda_{\text{som}}, \Lambda_1, \Lambda_2, L_1, L_2)$ to (2.1)–(2.5) in the sense of Definition 3.1.*

3.3. Proof of Theorem 3.2. The proof is based on a fixed point argument applied to an operator obtained by concatenating linearized versions of (2.2), (2.4), and (2.5). Let us briefly sketch our strategy. We work in the Banach space $X = \prod_{j=1,2} (L^2((0, T); H^1(0, L_j(t)))^2$ endowed with the norm

$$\|(\mathbf{f}_1, \mathbf{f}_2)\|_X^2 = \sum_{j=1,2} \sum_{i=+,-} \|f_{i,j}\|_{L^2((0,T);H^1(0,L_j(t)))}^2.$$

Let $(\widehat{\mathbf{f}}_1, \widehat{\mathbf{f}}_2) \in X$ be fixed and let $\mathbf{\Lambda} \in C^1([0, T])^3$ be the unique solution to the pure ODE system

$$\begin{aligned} \Lambda'_{\text{som}}(t) &= \sum_{j=1,2} (\beta_{-,j}(\Lambda_{\text{som}}(t)) \widehat{f}_{-,j}(t, 0) - \alpha_{+,j}(\Lambda_{\text{som}}(t)) g_{+,j}(\widehat{\mathbf{f}}_j(t, 0))) + \gamma_{\text{prod}}(t), \\ \Lambda'_1(t) &= \beta_{+,1}(\Lambda_1(t)) \widehat{f}_{+,1}(t, L_1(t)) - \alpha_{-,1}(\Lambda_1(t)) g_{-,1}(\widehat{\mathbf{f}}_1(t, L_1(t))) \\ &\quad - c_1 h_1(\Lambda_1(t), L_1(t)), \\ \Lambda'_2(t) &= \beta_{+,2}(\Lambda_2(t)) \widehat{f}_{+,2}(t, L_2(t)) - \alpha_{-,2}(\Lambda_2(t)) g_{-,2}(\widehat{\mathbf{f}}_2(t, L_2(t))) \\ &\quad - c_2 h_2(\Lambda_2(t), L_2(t)). \end{aligned} \tag{3.2}$$

Denote the mapping $(\widehat{\mathbf{f}}_1, \widehat{\mathbf{f}}_2) \mapsto \mathbf{\Lambda}$ by \mathcal{B}_1 . This $\mathbf{\Lambda}$ depends on $(\widehat{\mathbf{f}}_1, \widehat{\mathbf{f}}_2)$ and is now substituted into (2.4), that is, we are looking for the unique solution $\mathbf{L} \in C^1([0, T])^2$ to the pure ODE problem

$$L'_j(t) = h_j(\Lambda_j(t), L_j(t)), \tag{3.3}$$

whose solution operator is denoted by \mathcal{B}_2 . Then, such $\mathbf{\Lambda}$ and \mathbf{L} are substituted into (2.1)–(2.3), and we look for the unique solution $\mathbf{f}_j \in (L^2((0, T); H^1(0, L_j(t))))^2$, with $\partial_t \mathbf{f}_j \in (L^2((0, T); H^1(0, L_j(t))))^2$, to the pure PDE problem

$$\begin{aligned} & \int_0^{L_j(t)} \partial_t f_{+,j} \varphi_+ \, dx \\ &= \int_0^{L_j(t)} (v_0 f_{+,j}(1 - \rho_j) - D_T \partial_x f_{+,j}) \partial_x \varphi_+ + \lambda(f_{-,j} - f_{+,j}) \varphi_+ \, dx \\ & \quad - \beta_{+,j}(\Lambda_j) f_{+,j}(t, L_j(t)) \varphi_+(L_j(t)) + \alpha_{+,j}(\Lambda_{\text{som}}) g_{+,j}(\mathbf{f}_j(t, 0)) \varphi_+(0), \end{aligned} \quad (3.4)$$

$$\begin{aligned} & \int_0^{L_j(t)} \partial_t f_{-,j} \varphi_- \, dx \\ &= \int_0^{L_j(t)} -(v_0 f_{-,j}(1 - \rho_j) + D_T \partial_x f_{-,j}) \partial_x \varphi_- + \lambda(f_{+,j} - f_{-,j}) \varphi_- \, dx \\ & \quad + \alpha_{-,j}(\Lambda_j) g_{-,j}(\mathbf{f}_j(t, L_j(t))) \varphi_-(L_j(t)) - \beta_{-,j}(\Lambda_{\text{som}}(t)) f_{-,j}(t, 0) \varphi_-(0), \end{aligned} \quad (3.5)$$

for every $\varphi_+, \varphi_- \in H^1(0, L_j(t))$. We call \mathcal{B}_3 the solution operator $(\mathbf{\Lambda}, \mathbf{L}) \mapsto (\mathbf{f}_1, \mathbf{f}_2)$. Then, given an appropriate subset $\mathcal{K} \subset X$, we define the fixed point operator $\mathcal{B}: \mathcal{K} \rightarrow X$ such that

$$\mathcal{B}(\widehat{\mathbf{f}}_1, \widehat{\mathbf{f}}_2) = \mathcal{B}_3(\mathcal{B}_1(\widehat{\mathbf{f}}_1, \widehat{\mathbf{f}}_2), \mathcal{B}_2(\mathcal{B}_1(\widehat{\mathbf{f}}_1, \widehat{\mathbf{f}}_2))) = (\mathbf{f}_1, \mathbf{f}_2).$$

We show that \mathcal{B} is self-mapping and contractive so that existence is a consequence of the Banach's fixed point theorem.

Let us begin with system (3.2).

Lemma 3.3. *Let $(\widehat{\mathbf{f}}_1, \widehat{\mathbf{f}}_2) \in X$, then, there exists a unique $\mathbf{\Lambda} = (\Lambda_{\text{som}}, \Lambda_1, \Lambda_2) \in C^1([0, T])^3$ that solves (3.2) with initial conditions*

$$\Lambda_k(0) = \Lambda_k^0, \quad k = \text{som}, 1, 2. \quad (3.6)$$

Proof. This result is an application of the Cauchy-Lipschitz theorem, since the right-hand sides of (3.2) are Lipschitz continuous with respect to Λ_k thanks to hypotheses (H₄) and (H₅). \square

Lemma 3.4. *Let $\mathcal{B}_1: X \rightarrow C([0, T])^3$ be the operator that maps $(\widehat{\mathbf{f}}_1, \widehat{\mathbf{f}}_2) \in X$ to the solution $\mathbf{\Lambda}$ to (3.2). Then, \mathcal{B}_1 is Lipschitz continuous.*

Proof. From Lemma 3.3, \mathcal{B}_1 is well defined. Let now $(\widehat{\mathbf{f}}_1^{(1)}, \widehat{\mathbf{f}}_2^{(1)}), (\widehat{\mathbf{f}}_1^{(2)}, \widehat{\mathbf{f}}_2^{(2)}) \in X$ and let $\mathbf{\Lambda}^{(1)} =: \mathcal{B}_1(\widehat{\mathbf{f}}_1^{(1)}, \widehat{\mathbf{f}}_2^{(1)})$ and $\mathbf{\Lambda}^{(2)} =: \mathcal{B}_1(\widehat{\mathbf{f}}_1^{(2)}, \widehat{\mathbf{f}}_2^{(2)})$ be solutions to (3.2) satisfying the same initial condition (3.6). We fix $t \in [0, T]$ and consider

$$\begin{aligned} (\Lambda_j^{(a)})'(t) &= \beta_{+,j}(\Lambda_j^{(a)}(t)) \widehat{f}_{+,j}^{(a)}(t, L_j(t)) - \alpha_{-,j}(\Lambda_j^{(a)}(t)) g_{-,j}(\widehat{\mathbf{f}}_j^{(a)}(t, L_j(t))) \\ & \quad - c_j h_j(\Lambda_j^{(a)}(t), L_j(t)), \end{aligned}$$

$a = 1, 2$. Taking the difference of the two equations, setting $\delta \Lambda_j := \Lambda_j^{(1)} - \Lambda_j^{(2)}$, exploiting hypotheses (H₂)–(H₅) and summarizing the constants give

$$|(\delta \Lambda_j)'(t)| \leq C |\delta \Lambda_j(t)| + C \left(|(\widehat{f}_{+,j}^{(1)} - \widehat{f}_{+,j}^{(2)})(t, L_j(t))| + |(\widehat{f}_{-,j}^{(1)} - \widehat{f}_{-,j}^{(2)})(t, L_j(t))| \right),$$

while the trace inequality (3.1) and a Gronwall argument imply

$$|\Lambda_j^{(1)}(t) - \Lambda_j^{(2)}(t)| \leq C \|\widehat{\mathbf{f}}_j^{(1)} - \widehat{\mathbf{f}}_j^{(2)}\|_{L^2((0, T); H^1(0, L_j(t)))^2}.$$

A similar argument holds for the equation in Λ_{som} , and we eventually have

$$\|\mathbf{\Lambda}^{(1)} - \mathbf{\Lambda}^{(2)}\|_{C([0, T])^3} \leq C \|(\widehat{\mathbf{f}}_1^{(1)}, \widehat{\mathbf{f}}_2^{(1)}) - (\widehat{\mathbf{f}}_1^{(2)}, \widehat{\mathbf{f}}_2^{(2)})\|_X. \quad (3.7)$$

\square

We next show the following existence result for equation (3.3).

Lemma 3.5. *Let $\mathbf{\Lambda} \in C^1([0, T])^3$ be the unique solution to (3.2). Then, there exists a unique $\mathbf{L} = (L_1, L_2) \in C^1([0, T])^2$ that solves (3.3) with initial condition $L_j(0) = L_j^{(0)}$. Furthermore, for all $t \in (0, T)$ it holds*

$$\ell_j \leq L_j(t) \leq L_j^{(0)} + T \|h_j\|_{L^\infty(\mathbb{R}^2)} \quad (3.8)$$

$$\frac{|L_j'(t)|}{L_j(t)} \leq \frac{\|h_j\|_{L^\infty(\mathbb{R}^2)}}{\ell_j}. \quad (3.9)$$

Proof. The existence and uniqueness follow as before. Moreover, thanks to hypotheses (H₀) and (H₃)-(ii) and (iii), [8, Theorem 5.1] implies $L_j(t) \geq \ell_j$ for all $t \in (0, T)$. This gives the leftmost inequality of (3.8). In order to prove the right-most inequality, we fix $t \in (0, T)$, integrate (3.3), and use (H₃)-(i) to have

$$L_j(t) = L_j^{(0)} + \int_0^t h_j(\Lambda_j(s), L_j(s)) \, ds \leq L_j^{(0)} + T \|h_j\|_{L^\infty(\mathbb{R}^2)}.$$

In addition, we observe that (3.3) gives $|L_j'(t)| \leq \|h_j\|_{L^\infty(\mathbb{R}^2)}$. Then, the fact that $L_j(t) \geq \ell_j$ allows us to conclude (3.9). \square

Lemma 3.6. *The operator $\mathcal{B}_2: C([0, T])^3 \rightarrow C([0, T])^2$ that maps $\mathbf{\Lambda}$ to the solution \mathbf{L} to (3.3) is Lipschitz continuous in the sense of*

$$\|\mathbf{L}^{(1)} - \mathbf{L}^{(2)}\|_{C([0, T])^2} \leq T \max_{j=1,2} \{L_{h_j} e^{2TL_{h_j}}\} \|\mathbf{\Lambda}^{(1)} - \mathbf{\Lambda}^{(2)}\|_{C([0, T])^3}, \quad (3.10)$$

where L_{h_j} is the Lipschitz constant of h_j . If $T \max_{j=1,2} \{L_{h_j} e^{2TL_{h_j}}\} < 1$, then \mathcal{B}_2 is contractive.

Proof. The proof works as for Lemma 3.4 so we omit it. \square

We next investigate the existence of solutions to system (3.4)–(3.5).

Theorem 3.7. *Let $\mathbf{\Lambda}$ and \mathbf{L} be the unique solution to (3.2) and (3.3), respectively. Then, there exists a unique solution $(\mathbf{f}_1, \mathbf{f}_2) \in X$ to (3.4)–(3.5) such that $f_{i,j} \in [0, 1]$ for a.e. $x \in (0, L_j(t))$ and $t \in [0, T]$.*

Proof. To simplify the notation, for the proof of this result we will drop the use of the j -index and, for the reader's convenience, we split the proof in several steps.

Step 1: Change of variables. We first transform (3.4)–(3.5) into an equivalent system settled on a fixed domain. To this end, we make the following change of variables

$$y = y(t, x) =: \frac{x}{L(t)} \quad \longleftrightarrow \quad x = L(t)y.$$

Then we define the functions $\bar{f}_i(t, y) = f_i(t, x) = f_i(t, L(t)y)$, and observe that

$$\partial_x f_i = \frac{1}{L(t)} \partial_y \bar{f}_i \quad \partial_t f_i = \partial_t \bar{f}_i - L'(t) y \partial_x f_i = \partial_t \bar{f}_i - \frac{L'(t)}{L(t)} y \partial_y \bar{f}_i, \quad dx = L(t) dy. \quad (3.11)$$

Using (3.11) in (3.4) and rearranging gives

$$\begin{aligned} & \int_0^1 \partial_t \bar{f}_+ \bar{\varphi}_+ \, dy + \frac{D_T}{L^2(t)} \int_0^1 \partial_y \bar{f}_+ \partial_y \bar{\varphi}_+ \, dy \\ &= \int_0^1 \frac{v_0}{L(t)} \bar{f}_+ (1 - \bar{\rho}) \partial_y \bar{\varphi}_+ + \left(\lambda(\bar{f}_- - \bar{f}_+) + \frac{L'(t)}{L(t)} y \partial_y \bar{f}_+ \right) \bar{\varphi}_+ \, dy \\ & \quad - \beta_+(\mathbf{\Lambda}) \bar{f}_+(t, 1) \bar{\varphi}_+(1) + \alpha_+(\mathbf{\Lambda}_{\text{som}}) g_+(\bar{\mathbf{f}}(t, 0)) \bar{\varphi}_+(0), \end{aligned} \quad (3.12)$$

and the same holds for (3.5) so that the sum reads as (after omitting the bar symbols)

$$\begin{aligned}
& \sum_{i=+,-} \int_0^1 \partial_t f_i \varphi_i \, dy + \frac{D_T}{L^2(t)} \sum_{i=+,-} \int_0^1 \partial_y f_i \partial_y \varphi_i \, dy \\
&= \sum_{i=+,-} \int_0^1 \frac{L'(t)}{L(t)} y \partial_y f_i \varphi_i \, dy + \int_0^1 \frac{v_0}{L(t)} f_+ (1 - \rho) \partial_y \varphi_+ + \lambda(f_- - f_+) \varphi_+ \, dy \\
&+ \int_0^1 -\frac{v_0}{L(t)} f_- (1 - \rho) \partial_y \varphi_- + \lambda(f_+ - f_-) \varphi_- \, dy - \beta_+(\Lambda) f_+(t, 1) \varphi_+(1) \\
&+ \alpha_+(\Lambda_{\text{som}}) g_+(\mathbf{f}(t, 0)) \varphi_+(0) + \alpha_-(\Lambda) g_-(\mathbf{f}(t, 1)) \varphi_-(1) - \beta_-(\Lambda_{\text{som}}) f_-(t, 0) \varphi_-(0).
\end{aligned} \tag{3.13}$$

Step 2: The truncation. Given a generic function a we introduce the truncation

$$a_{\text{tr}} = \begin{cases} a & \text{if } 0 \leq a \leq 1, \\ 0 & \text{otherwise,} \end{cases} \tag{3.14}$$

and then consider the following truncated version of (3.13)

$$\begin{aligned}
& \sum_{i=+,-} \int_0^1 \partial_t f_i \varphi_i \, dy + \frac{D_T}{L^2(t)} \sum_{i=+,-} \int_0^1 \partial_y f_i \partial_y \varphi_i \, dy \\
&= \sum_{i=+,-} \int_0^1 \frac{L'(t)}{L(t)} y \partial_y f_i \varphi_i \, dy + \int_0^1 \frac{v_0}{L(t)} (f_+ (1 - \rho))_{\text{tr}} \partial_y \varphi_+ + \lambda(f_- - f_+) \varphi_+ \, dy \\
&+ \int_0^1 -\frac{v_0}{L(t)} (f_- (1 - \rho))_{\text{tr}} \partial_y \varphi_- + \lambda(f_+ - f_-) \varphi_- \, dy - \beta_+(\Lambda) f_+(t, 1) \varphi_+(1) \\
&+ \alpha_+(\Lambda_{\text{som}}) g_+(\mathbf{f}(t, 0)) \varphi_+(0) + \alpha_-(\Lambda) g_-(\mathbf{f}(t, 1)) \varphi_-(1) - \beta_-(\Lambda_{\text{som}}) f_-(t, 0) \varphi_-(0).
\end{aligned} \tag{3.15}$$

We solve (3.15) by means of the Banach fixed point theorem. We follow [9], pointing out that a similar approach has been used also in [16], yet in a different context.

Let us set $Y := (L^\infty((0, T); L^2(0, 1)))^2$ and introduce the following nonempty, closed set

$$\mathcal{M} = \{\mathbf{f} = (f_+, f_-) \in Y : \|\mathbf{f}\|_Y \leq C_{\mathcal{M}}\},$$

with $T, C_{\mathcal{M}} > 0$ to be specified. Then we define the mapping $\Phi: \mathcal{M} \rightarrow Y$ such that $\Phi(\tilde{\mathbf{f}}) = \mathbf{f}$, where, for fixed $\tilde{\mathbf{f}} \in \mathcal{M}$, \mathbf{f} solves the following linearized equation [15, Chapter III]

$$\begin{aligned}
& \sum_{i=+,-} \int_0^1 \partial_t f_i \varphi_i \, dy + \frac{D_T}{L^2(t)} \sum_{i=+,-} \int_0^1 \partial_y f_i \partial_y \varphi_i \, dy \\
&= \sum_{i=+,-} \int_0^1 \frac{L'(t)}{L(t)} y \partial_y f_i \varphi_i \, dy + \int_0^1 \frac{v_0}{L(t)} (\tilde{f}_+ (1 - \tilde{\rho}))_{\text{tr}} \partial_y \varphi_+ + \lambda(f_- - f_+) \varphi_+ \, dy \\
&+ \int_0^1 -\frac{v_0}{L(t)} (\tilde{f}_- (1 - \tilde{\rho}))_{\text{tr}} \partial_y \varphi_- + \lambda(f_+ - f_-) \varphi_- \, dy - \beta_+(\Lambda) f_+(t, 1) \varphi_+(1) \\
&+ \alpha_+(\Lambda_{\text{som}}) g_+(\tilde{\mathbf{f}}(t, 0)) \varphi_+(0) + \alpha_-(\Lambda) g_-(\tilde{\mathbf{f}}(t, 1)) \varphi_-(1) - \beta_-(\Lambda_{\text{som}}) f_-(t, 0) \varphi_-(0).
\end{aligned} \tag{3.16}$$

Step 3: Φ is self-mapping. We show that

$$\|\mathbf{f}\|_Y \leq C_{\mathcal{M}}. \tag{3.17}$$

We choose $\varphi_i = f_i$ in (3.16) and estimate the several terms appearing in the resulting equation separately. From (3.8), on the left-hand side we have

$$\begin{aligned} & \frac{1}{2} \frac{d}{dt} \sum_{i=+,-} \int_0^1 |f_i|^2 dy + \frac{D_T}{L^2(t)} \sum_{i=+,-} \int_0^1 |\partial_y f_i|^2 dy \\ & \geq \frac{1}{2} \frac{d}{dt} \sum_{i=+,-} \int_0^1 |f_i|^2 dy + \frac{D_T}{(L^{(0)} + T\|h\|_{L^\infty(\mathbb{R})})^2} \sum_{i=+,-} \int_0^1 |\partial_y f_i|^2 dy. \end{aligned}$$

On the right-hand side we first use equation (3.9) along with Young's inequality for some $\varepsilon_1 > 0$ and the fact that $y \in (0, 1)$ to achieve

$$\sum_{i=+,-} \int_0^1 \frac{L'(t)}{L(t)} y f_i \partial_y f_i dy \leq \sum_{i=+,-} \left(\varepsilon_1 \|\partial_y f_i\|_{L^2(0,1)}^2 + \frac{\|h\|_{L^\infty(\mathbb{R})}^2}{\varepsilon_1 \ell^2} \|f_i\|_{L^2(0,1)}^2 \right).$$

On the other hand, (3.8), Young's inequality for some $\varepsilon_2 > 0$ and (3.14) give

$$\pm \int_0^1 \frac{v_0}{L(t)} (\tilde{f}_i(1 - \tilde{\rho}))_{\text{tr}} \partial_y f_i dy \leq C + \varepsilon_2 \|\partial_y f_i\|_{L^2(0,1)}^2.$$

We further observe that

$$\lambda \int_0^1 (f_- - f_+) f_+ + (f_+ - f_-) f_- dy = -\lambda \int_0^1 (f_+ + f_-)^2 dy \leq 0.$$

Finally we estimate the boundary terms. We use again Young's inequality with some $\varepsilon_3, \dots, \varepsilon_6 > 0$ and the trace inequality (3.1) to achieve

$$\begin{aligned} \beta_+(\Lambda) f_+^2(t, 1) &\leq C \|f_+\|_{L^2(0,1)}^2 + \varepsilon_3 \|\partial_y f_+\|_{L^2(0,1)}^2, \\ \alpha_+(\Lambda_{\text{som}}) g_+(\tilde{\mathbf{f}}_+(t, 0)) f_+(t, 0) &\leq C \|f_+\|_{L^2(0,1)}^2 + \varepsilon_4 \|\partial f_+\|_{L^2(0,1)}^2, \\ \alpha_-(\Lambda) g_-(\tilde{\mathbf{f}}_+(t, 1)) f_-(t, 1) &\leq C \|f_-\|_{L^2(0,1)}^2 + \varepsilon_5 \|\partial_y f_-\|_{L^2(0,1)}^2, \\ \beta_-(\Lambda_{\text{som}}) f_-^2(t, 0) &\leq C \|f_-\|_{L^2(0,1)}^2 + \varepsilon_6 \|\partial_y f_-\|_{L^2(0,1)}^2. \end{aligned}$$

We choose $\varepsilon_\kappa, \kappa = 1, \dots, 6$, in such a way that all the terms of the form $\|\partial_y f_i\|_{L^2(0,1)}$ can be absorbed on the left-hand side of (3.16), which simplifies to

$$\frac{d}{dt} \sum_{i=+,-} \int_0^1 |f_i|^2 dy \leq C \sum_{i=+,-} \|f_i\|_{L^2(0,1)}^2 + C.$$

We then use a Gronwall argument to infer

$$\sup_{t \in (0, T)} \|f_i(t, \cdot)\|_{L^2(0,1)}^2 \leq C.$$

Choosing $C_{\mathcal{M}} := \tilde{C}^{1/2}$ implies that (3.17) is satisfied and therefore Φ is self-mapping.

Step 4: Φ is a contraction. Let $\tilde{\mathbf{f}}_1, \tilde{\mathbf{f}}_2 \in \mathcal{M}$ and let $\mathbf{f}_1 =: \Phi(\tilde{\mathbf{f}}_1)$ and $\mathbf{f}_2 =: \Phi(\tilde{\mathbf{f}}_2)$ be two solutions to (3.16) with the same initial datum \mathbf{f}^0 . We then consider the difference of the corresponding equations and choose $\varphi_i = f_{i,1} - f_{i,2}$. Reasoning as in Step 2 and exploiting the Lipschitz continuity of the functions

$$\mathbb{R}^2 \ni (a, b) \mapsto (a(1 - a - b))_{\text{tr}} \quad \text{and} \quad \mathbb{R}^2 \ni (a, b) \mapsto (b(1 - a - b))_{\text{tr}} \quad (3.18)$$

we get

$$\frac{d}{dt} \sum_{i=+,-} \|f_{i,1} - f_{i,2}\|_{L^2(0,1)}^2 \leq C \sum_{i=+,-} \left(\|f_{i,1} - f_{i,2}\|_{L^2(0,1)}^2 + \|\tilde{f}_{i,1} - \tilde{f}_{i,2}\|_{L^2(0,1)}^2 \right).$$

Again by means of a Gronwall argument we have

$$\sum_{i=+,-} \|f_{i,1} - f_{i,2}\|_{L^\infty((0,T);L^2(0,1))}^2 \leq CT e^{CT} \sum_{i=+,-} \|\tilde{f}_{i,1} - \tilde{f}_{i,2}\|_{L^\infty((0,T);L^2(0,1))}^2,$$

and then Φ is a contraction if $T > 0$ is small enough so that $CTe^{CT} < 1$. Then Banach's fixed point theorem applies and we obtain a solution $\mathbf{f} \in (L^\infty((0, T); L^2(0, 1)))^2$ to (3.15). A standard regularity theory then gives $\mathbf{f} \in (L^2((0, T); H^1(0, 1)))^2$, with $\partial_t \mathbf{f} \in (L^2((0, T); H^1(0, 1)'))^2$.

Step 5: Box constraints. We show that such \mathbf{f} obtained in Step 4 is actually a solution to (3.13), because it satisfies the box constraint $f_+, f_- \geq 0$ and $\rho \leq 1$.

We start by showing that $f_+ \geq 0$, and to this end we consider only the terms involving the φ_+ -functions in (3.15), that is,

$$\begin{aligned} & \int_0^1 \partial_t f_+ \varphi_+ \, dy + \frac{D_T}{L^2(t)} \int_0^1 \partial_y f_+ \partial_y \varphi_+ \, dy \\ &= \int_0^1 \frac{v_0}{L(t)} (f_+ (1 - \rho))_{\text{tr}} \partial_y \varphi_+ + \left(\lambda(f_- - f_+) + \frac{L'(t)}{L(t)} y \partial_y f_+ \right) \varphi_+ \, dy \\ & \quad - \beta_+(\Lambda) f_+(t, 1) \varphi_+(1) + \alpha_+(\Lambda_{\text{som}}) g_+(\mathbf{f}(t, 0)) \varphi_+(0). \end{aligned} \quad (3.19)$$

For every $\varepsilon > 0$ we consider the function $\eta_\varepsilon \in W^{2,\infty}(\mathbb{R})$ given by

$$\eta_\varepsilon(u) = \begin{cases} 0 & \text{if } u \leq 0, \\ \frac{u^2}{4\varepsilon} & \text{if } 0 < u \leq 2\varepsilon, \\ u - \varepsilon & \text{if } u > 2\varepsilon. \end{cases} \quad \text{with} \quad \eta_\varepsilon''(u) = \begin{cases} 0 & \text{if } u \leq 0, \\ \frac{1}{2\varepsilon} & \text{if } 0 < u \leq 2\varepsilon, \\ 0 & \text{if } u > 2\varepsilon. \end{cases} \quad (3.20)$$

Next we choose $\varphi_+ = -\eta_\varepsilon'(-f_+)$ and observe that by the chain rule we have $\partial_y \varphi_+ = \eta_\varepsilon''(-f_+) \partial_y f_+$. Using such φ_+ in (3.19) gives

$$\begin{aligned} & - \int_0^1 \partial_t f_+ \eta_\varepsilon'(-f_+) \, dy + \frac{D_T}{L(t)^2} \int_0^1 \eta_\varepsilon''(-f_+) |\partial_y f_+|^2 \, dy \\ &= \int_0^1 \frac{v_0}{L(t)} (f_+ (1 - \rho))_{\text{tr}} \eta_\varepsilon''(-f_+) \partial_y f_+ - \left(\lambda(f_- - f_+) + \frac{L'(t)}{L(t)} y \partial_y f_+ \right) \eta_\varepsilon'(-f_+) \, dy \\ & \quad + \beta_+(\Lambda) f_+(t, 1) \eta_\varepsilon'(-f_+(t, 1)) - \alpha_+(\Lambda_{\text{som}}) g_+(\mathbf{f}(t, 0)) \eta_\varepsilon'(-f_+(t, 0)). \end{aligned}$$

Thanks to Young's inequality with a suitable $\kappa > 0$ and to (3.14) we have

$$\begin{aligned} & \int_0^1 \frac{v_0}{L(t)} (f_+(1 - \rho))_{\text{tr}} \eta_\varepsilon''(-f_+) \partial_y f_+ \, dy \\ & \leq \kappa \int_0^1 \eta_\varepsilon''(-f_+) |\partial_y f_+|^2 \, dy + \frac{1}{\kappa} \int_0^1 \eta_\varepsilon''(-f_+) \left(\frac{v_0}{L(t)} \right)^2 (f_+(1 - \rho))_{\text{tr}}^2 \, dy. \end{aligned}$$

Choosing κ sufficiently small and simplifying give

$$\begin{aligned} & \frac{d}{dt} \int_0^1 \eta_\varepsilon(-f_+) \, dy = - \int_0^1 \partial_t f_+ \eta_\varepsilon'(-f_+) \, dy \\ & \leq \int_0^1 C \eta_\varepsilon''(-f_+) \left(\frac{v_0}{L(t)} \right)^2 (f_+(1 - \rho))_{\text{tr}}^2 - \left(\lambda(f_- - f_+) + \frac{L'(t)}{L(t)} y \partial_y f_+ \right) \eta_\varepsilon'(-f_+) \, dy \\ & \quad + \beta_+(\Lambda) f_+(t, 1) \eta_\varepsilon'(-f_+(t, 1)). \end{aligned} \quad (3.21)$$

To gain some sign information on the right-hand side of (3.21), we introduce the set

$$\Omega_\varepsilon := \{y \in (0, 1) : 0 < f_+(t, y), f_-(t, y) \leq 2\varepsilon\}. \quad (3.22)$$

We first use (3.8), (3.20), and the Lipschitz continuity of (3.18) to have

$$\begin{aligned} & \int_{\Omega_\varepsilon} \eta_\varepsilon''(-f_+) \left(\frac{v_0}{L(t)} \right)^2 ((f_+(1 - \rho))_{\text{tr}})^2 \, dy \\ &= \int_{\Omega_\varepsilon} \eta_\varepsilon''(-f_+) \left(\frac{v_0}{L(t)} \right)^2 ((f_+(1 - \rho))_{\text{tr}} - (0 \cdot (1 - \rho))_{\text{tr}})^2 \, dy \leq \frac{v_0^2}{\ell^2} 2\varepsilon |\Omega_\varepsilon| =: \tilde{c}_1 \varepsilon. \end{aligned}$$

On the other hand, from (3.22) it follows that $-2\varepsilon < f_+ - f_- \leq 2\varepsilon$, which implies

$$-\int_{\Omega_\varepsilon} \lambda(f_- - f_+) \, dy \leq 2\varepsilon \lambda |\Omega_\varepsilon| =: \tilde{c}_2 \varepsilon.$$

Concerning the boundary term, we note that by definition the function η'_ε is nonzero only if its argument is nonnegative, which in any case gives

$$\beta_+(\Lambda) f_+(t, 1) \eta'_\varepsilon(-f_+(t, 1)) \leq 0.$$

Finally, since $-\partial_y f_+ \eta'_\varepsilon(-f_+) = \partial_y \eta_\varepsilon(-f_+)$, we can use an integration by parts and exploit the fact that the function η_ε has a sign to have

$$-\int_0^1 y \partial_y f_+ \eta'_\varepsilon(-f_+) \, dy = \eta_\varepsilon(-f_+(t, 1)) - \int_0^1 \eta_\varepsilon(-f_+) \, dy \leq \int_0^1 \eta_\varepsilon(-f_+) \, dy,$$

where in the last inequality we observe that the term $\eta_\varepsilon(-f_+(t, 1))$ is significant only if $-f_+(t, 1) > 0$. Gathering all these information gives that (3.21) simplifies to

$$\frac{d}{dt} \int_0^1 \eta_\varepsilon(-f_+) \, dy \leq C \int_0^1 \eta_\varepsilon(-f_+) \, dy + C\varepsilon.$$

A Gronwall argument then gives

$$\int_0^1 \eta_\varepsilon(-f_+(t, \cdot)) \, dy \leq e^t \left(C\varepsilon t + \int_0^1 \eta_\varepsilon(-f_+^0) \, dy \right).$$

Passing to the limit as $\varepsilon \rightarrow 0$ gives

$$0 \leq \int_0^1 (f_+)^- \, dy \leq e^t \int_0^1 (f_+^0)^- \, dy = 0,$$

where the last passage holds thanks to (H₁). Then $f_+ \geq 0$ as well.

The proof that $f_- \geq 0$ works in a similar way, starting again from equation (3.15) and taking into account only the terms involving the φ_- -functions.

We now show that $\rho \leq 1$ and then start from (3.15) with $\varphi_i := \varphi$. This gives

$$\begin{aligned} & \int_0^1 \partial_t \rho \varphi \, dy + \frac{D_T}{L^2(t)} \int_0^1 \partial_y \rho \partial_y \varphi \, dy \\ &= \int_0^1 \frac{L'(t)}{L(t)} y \partial_y \rho \varphi \, dy + \frac{v_0}{L(t)} \int_0^1 ((f_+(1-\rho))_{\text{tr}} - (f_-(1-\rho))_{\text{tr}}) \partial_y \varphi \, dy \\ & \quad - (\beta_+(\Lambda) f_+(t, 1) - \alpha_-(\Lambda) g_-(\mathbf{f}(t, 1))) \varphi(1) \\ & \quad - (\beta_-(\Lambda_{\text{som}}) f_-(t, 0) - \alpha_+(\Lambda_{\text{som}}) g_+(\mathbf{f}(t, 0))) \varphi(0). \end{aligned}$$

We choose $\varphi = \eta'_\varepsilon(\rho - 1)$, $\tilde{\Omega}_\varepsilon = \{y \in (0, 1) : 1 \leq \rho(t, y) \leq 1 + 2\varepsilon\}$, and reason as before exploiting hypothesis (H₂). Then the limit as $\varepsilon \rightarrow 0$ entails

$$0 \leq \int_0^1 (\rho - 1)^+ \, dy \leq \int_0^1 (\rho^0 - 1)^+ \, dy = 0,$$

thanks again to (H₁). It follows that is $\rho \leq 1$, then the claim is proved.

Step 6: Conclusion. Using the original notation, we have shown the existence of a solution $\bar{\mathbf{f}}$ to (3.13) such that $\bar{f}_+, \bar{f}_- \geq 0$ and $\bar{\rho} \leq 1$ for a.e. $y \in (0, 1)$, $t \in [0, T]$. This implies that \mathbf{f} is a weak solution to (3.4)–(3.5) such that $f_+, f_- \geq 0$ and $\rho \leq 1$ for a.e. $x \in (0, L(t))$, $t \in [0, T]$. The system is completely solved. \square

Lemma 3.8. *Let $\mathcal{B}_3 : C([0, T])^3 \times C([0, T])^2 \rightarrow X$ be the operator that maps $(\mathbf{\Lambda}, \mathbf{L})$ to the unique solution $(\mathbf{f}_1, \mathbf{f}_2)$ to (3.4)–(3.5). Then, \mathcal{B}_3 is Lipschitz continuous.*

Proof. Thanks to Theorem 3.7, \mathcal{B}_3 is well defined. We choose $\mathbf{\Lambda}^{(a)} \in C([0, T])^3$ and $\mathbf{L}^{(a)} \in C([0, T])^2$ and set $(\mathbf{f}_1^{(a)}, \mathbf{f}_2^{(a)}) =: \mathcal{B}_3(\mathbf{\Lambda}^{(a)}, \mathbf{L}^{(a)})$, $a = 1, 2$. Then using an argument similar as the one for Lemma 3.4 which this time applies also the change of variables (3.11) and a Gronwall inequality we have $a = 1, 2$.

$$\|(\mathbf{f}_1^{(1)}, \mathbf{f}_2^{(1)}) - (\mathbf{f}_1^{(2)}, \mathbf{f}_2^{(2)})\|_X^2 \leq \bar{C} e^{CT} \left(\|\mathbf{\Lambda}^{(1)} - \mathbf{\Lambda}^{(2)}\|_{C([0, T])^3}^2 + \|\mathbf{L}^{(1)} - \mathbf{L}^{(2)}\|_{C([0, T])^2}^2 \right), \quad (3.23)$$

with \bar{C} depending on $\|f_{i,j}^{(2)}\|_{L^2((0, T); H^1(0, 1))}$. The thesis follows. \square

Remark 3.9. We can recover a uniform bound for the constant \bar{C} appearing in (3.23). Indeed, starting from equation (3.12) and choosing as test functions first $f_{+,1}^{(2)}$ and then $f_{+,2}^{(2)}$ (with a similar argument for the equation involving the $f_{-,j}^{(2)}$'s) gives $\|f_{i,j}^{(2)}\|_{L^2((0, T); H^1(0, 1))} \leq CT e^{CT}$, uniformly. Then (3.23) reads as

$$\|(\mathbf{f}_1^{(1)}, \mathbf{f}_2^{(1)}) - (\mathbf{f}_1^{(2)}, \mathbf{f}_2^{(2)})\|_X^2 \leq CT e^{2CT} \left(\|\mathbf{\Lambda}^{(1)} - \mathbf{\Lambda}^{(2)}\|_{C([0, T])^3}^2 + \|\mathbf{L}^{(1)} - \mathbf{L}^{(2)}\|_{C([0, T])^2}^2 \right), \quad (3.24)$$

where now the constants depend only on the data.

3.4. Proof of Theorem 3.2. We use the Banach fixed point theorem to show the existence of a unique solution $(\mathbf{f}_1, \mathbf{f}_2, \mathbf{\Lambda}, \mathbf{L})$ to (2.1)–(2.5). We consider the set

$$\mathcal{K} = \{(\mathbf{f}_1, \mathbf{f}_2) \in X : 0 \leq f_{i,j}(t, x) \leq 1 \text{ for a.e. } x \in (0, L_j(t)) \text{ and } t \in [0, T]\}.$$

Let $\mathcal{B}: \mathcal{K} \rightarrow X$ be given by $\mathcal{B}(\mathbf{f}_1^{(1)}, \mathbf{f}_2^{(1)}) = \mathcal{B}_3(\mathcal{B}_1(\mathbf{f}_1^{(1)}, \mathbf{f}_2^{(1)}), \mathcal{B}_2(\mathcal{B}_1(\mathbf{f}_1^{(1)}, \mathbf{f}_2^{(1)})))$, where $\mathcal{B}_1, \mathcal{B}_2, \mathcal{B}_3$ are defined in Lemmas 3.4, 3.6, and 3.8, respectively. It holds that \mathcal{B} is well defined, while Theorem 3.7 implies that \mathcal{B} is self-mapping, that is, $\mathcal{B}: \mathcal{K} \rightarrow \mathcal{K}$.

We next show that \mathcal{B} is a contraction. Let $(\widehat{\mathbf{f}}_1^{(1)}, \widehat{\mathbf{f}}_2^{(1)}), (\widehat{\mathbf{f}}_1^{(2)}, \widehat{\mathbf{f}}_2^{(2)}) \in \mathcal{K}$ and set $(\mathbf{f}_1^{(1)}, \mathbf{f}_2^{(1)}) := \mathcal{B}(\widehat{\mathbf{f}}_1^{(1)}, \widehat{\mathbf{f}}_2^{(1)})$ as well as $(\mathbf{f}_1^{(2)}, \mathbf{f}_2^{(2)}) := \mathcal{B}(\widehat{\mathbf{f}}_1^{(2)}, \widehat{\mathbf{f}}_2^{(2)})$. Using (3.24), (3.10), and (3.7), and summarizing the not essential constants gives

$$\|(\mathbf{f}_1^{(1)}, \mathbf{f}_2^{(1)}) - (\mathbf{f}_1^{(2)}, \mathbf{f}_2^{(2)})\|_X \leq CT e^{CT} \|(\widehat{\mathbf{f}}_1^{(1)}, \widehat{\mathbf{f}}_2^{(1)}) - (\widehat{\mathbf{f}}_1^{(2)}, \widehat{\mathbf{f}}_2^{(2)})\|_X,$$

from which the contractivity follows if $T > 0$ is small enough that $CT e^{CT} < 1$. Thanks to the Banach's fixed point theorem we then infer the existence of a unique $(\mathbf{f}_1, \mathbf{f}_2) \in \mathcal{K}$ such that $(\mathbf{f}_1, \mathbf{f}_2) = \mathcal{B}(\mathbf{f}_1, \mathbf{f}_2)$. Observe that, from (3.7) and (3.10), this implies the uniqueness of $\mathbf{\Lambda}$ and \mathbf{L} , respectively. Due to the uniform L^∞ -bounds on \mathbf{f}_j , a concatenation argument yields existence on the complete interval $[0, T]$. The proof is thus complete.

4. STATIONARY SOLUTIONS

This section is dedicated to a brief investigation of stationary solutions $(\mathbf{f}_1^\infty, \mathbf{f}_2^\infty, \mathbf{\Lambda}^\infty, \mathbf{L}^\infty)$ to (2.1)–(2.5). That is, they satisfy

$$\begin{aligned} 0 &= -\partial_x [v_0 f_{+,j}^\infty (1 - \rho_j^\infty) - D_T \partial_x f_{+,j}^\infty] + \lambda(f_{-,j}^\infty - f_{+,j}^\infty), \\ 0 &= -\partial_x [-v_0 f_{-,j}^\infty (1 - \rho_j^\infty) - D_T \partial_x f_{-,j}^\infty] + \lambda(f_{+,j}^\infty - f_{-,j}^\infty), \end{aligned} \quad \text{in } (0, L_j^\infty), \quad (4.1)$$

with boundary conditions

$$\begin{aligned} J_{+,j}^\infty(0) &= \alpha_{+,j}(\Lambda_{\text{som}}^\infty) g_{+,j}(\mathbf{f}_j^\infty(0)), & -J_{-,j}^\infty(0) &= \beta_{-,j}(\Lambda_{\text{som}}^\infty) f_{-,j}^\infty(0), \\ J_{+,j}^\infty(L_j^\infty) &= \beta_{+,j}(\Lambda_j^\infty) f_{+,j}^\infty(L_j^\infty), & -J_{-,j}^\infty(L_j^\infty) &= \alpha_{-,j}(\Lambda_j^\infty) g_{-,j}(\mathbf{f}_j^\infty(L_j^\infty)), \end{aligned} \quad (4.2)$$

while $\mathbf{\Lambda}^\infty$ and \mathbf{L}^∞ solve

$$\begin{aligned} 0 &= \sum_{j=1,2} (\beta_{-,j}(\Lambda_{\text{som}}^\infty) f_{-,j}^\infty(0) - \alpha_{+,j}(\Lambda_{\text{som}}^\infty) g_{+,j}(\mathbf{f}_j^\infty(0))), \\ 0 &= \beta_{+,j}(\Lambda_j^\infty) f_{+,j}^\infty(L_j^\infty) - \alpha_{-,j}(\Lambda_j^\infty) g_{-,j}(\mathbf{f}_j^\infty(L_j^\infty)) - c_j h_j(\Lambda_j^\infty, L_j^\infty), \\ 0 &= h_j(\Lambda_j^\infty, L_j^\infty), \end{aligned} \quad (4.3)$$

respectively. Notice that we assumed $\gamma(t) \rightarrow 0$ as $t \rightarrow \infty$, cf. hypothesis (H₇), in order to guarantee a finite total mass of the stationary state. From the modelling point of view, this means that at the end of the growth phase, when the neuron is fully developed, there is no more production of vesicles in the

soma. In addition to equations (4.1)–(4.3), stationary solutions are parametrized by their total mass $m_\infty := \sum_{j=1,2} \left(\int_0^{L_j^\infty} \rho_j^\infty(x) dx + \Lambda_j^\infty \right) + \Lambda_{\text{som}}^\infty$.

For fixed $m_\infty > 0$, we expect three possible types of stationary solutions:

- No mass inside the neurites, i.e., $\rho_j^\infty = 0$, and $m_\infty = \Lambda_1^\infty + \Lambda_2^\infty + \Lambda_{\text{som}}^\infty$. This solution is always possible as it automatically satisfies (4.2). The length depends on the fraction of mass stored in each Λ_j , which yields a family of infinite solutions.
- Constant solutions with mass inside the neurites, i.e., $\mathbf{f}_j^\infty \neq (0, 0)$. In this case, for $\lambda > 0$, the reaction term enforces $f_{-,j}^\infty = f_{+,j}^\infty =: f_j^\infty$. However, such solutions only exist if the nonlinearities at the boundary satisfy conditions so that (4.2) holds. In this case, compatibility with a given total mass m_∞ can be obtained by adjusting the concentration $\Lambda_{\text{som}}^\infty$, which decouples from the remaining equations.
- Non-constant solutions, featuring boundary layers at the end of the neurites.

A natural question is the existence of non-constant stationary solutions as well as their uniqueness and stability properties which we postpone to future work. Instead, we focus on conditions for the existence of non-trivial constant solutions.

4.1. Constant stationary solutions. We assume a strictly positive reaction rate $\lambda > 0$ which requires $f_{+,j} = f_{-,j} =: f_j^\infty \in [0, 1]$. Thus (4.1) reads as

$$0 = \partial_x [v_0 f_j^\infty (1 - \rho_j^\infty)] \quad \text{in } (0, L_j^\infty),$$

while the fluxes take the form

$$J_{+,j}^\infty = -J_{-,j}^\infty = v_0 f_j^\infty (1 - \rho_j^\infty) = v_0 f_j^\infty (1 - 2f_j^\infty). \quad (4.4)$$

Making the choice

$$g_{+,j}(f_{+,j}, f_{-,j}) = f_{+,j}(1 - \rho_j) \quad \text{as well as} \quad g_{-,j}(f_{+,j}, f_{-,j}) = f_{-,j}(1 - \rho_j), \quad (4.5)$$

the boundary conditions (4.2) become

$$\begin{aligned} J_{+,j}^\infty &= \alpha_{+,j}(\Lambda_{\text{som}}^\infty) f_j^\infty (1 - \rho_j^\infty) = \beta_{+,j}(\Lambda_j^\infty) f_j^\infty, \\ -J_{-,j}^\infty &= \alpha_{-,j}(\Lambda_j^\infty) f_j^\infty (1 - \rho_j^\infty) = \beta_{-,j}(\Lambda_{\text{som}}^\infty) f_j^\infty, \end{aligned} \quad (4.6)$$

which together with (4.4) yield

$$\alpha_{+,j}(\Lambda_{\text{som}}^\infty) = \alpha_{-,j}(\Lambda_j^\infty) = v_0 \quad \text{as well as} \quad \beta_{-,j}(\Lambda_{\text{som}}^\infty) = \beta_{+,j}(\Lambda_j^\infty) = v_0(1 - \rho_j^\infty).$$

Thus, fixing the values of f_j^∞ , we obtain Λ_j^∞ , $\Lambda_{\text{som}}^\infty$ by inverting $\alpha_{+,j}$, $\alpha_{-,j}$, $\beta_{+,j}$, and $\beta_{-,j}$, respectively, together with the compatibility condition

$$\alpha_{-,j}(\Lambda_j^\infty)(1 - \rho_j^\infty) = \beta_{+,j}(\Lambda_j^\infty) \quad \text{as well as} \quad \alpha_{+,j}(\Lambda_{\text{som}}^\infty)(1 - \rho_j^\infty) = \beta_{-,j}(\Lambda_{\text{som}}^\infty).$$

We further observe that the equations in (4.3) are the differences of in- and outflow at the respective boundaries, which in the case of constant f_j^∞ -s read as

$$\begin{aligned} 0 &= \sum_{j=1,2} (\beta_{-,j}(\Lambda_{\text{som}}^\infty) f_j^\infty - \alpha_{+,j}(\Lambda_{\text{som}}^\infty) f_j^\infty (1 - \rho_j^\infty)), \\ 0 &= \beta_{+,j}(\Lambda_j^\infty) f_j^\infty - \alpha_{-,j}(\Lambda_j^\infty) f_j^\infty (1 - \rho_j^\infty) - c_j h_j(\Lambda_j^\infty, L_j^\infty). \end{aligned} \quad (4.7)$$

It turns out that (4.7) will be automatically satisfied as soon as (4.6) and (4.3) hold. In particular, the last equation in (4.3) will determine the values of L_j^∞ . We make the choices

$$\beta_{+,j}(s) = c_{\beta_{+,j}} \left(1 - \frac{s}{\Lambda_{j,\text{max}}} \right), \quad \beta_{-,j}(s) = c_{\beta_{-,j}} \left(1 - \frac{s}{\Lambda_{\text{som,max}}} \right), \quad (4.8)$$

$$\alpha_{+,j}(s) = c_{\alpha_{+,j}} \frac{s}{\Lambda_{\text{som,max}}}, \quad \alpha_{-,j}(s) = c_{\alpha_{-,j}} \frac{s}{\Lambda_{j,\text{max}}}, \quad (4.9)$$

for some $c_{\beta_{i,j}}, c_{\alpha_{i,j}} \geq 0$, with $\Lambda_{\text{som,max}}, \Lambda_{j,\text{max}}$ the maximal capacity of soma and growth cones. Then, for given $f_j^\infty \in (0, \frac{1}{2}]$ to be a stationary solution, we need

$$\begin{aligned} c_{\alpha_{+,j}} &= v_0 \frac{\Lambda_{\text{som,max}}}{\Lambda_{\text{som}}^\infty}, & c_{\beta_{-,j}} &= v_0 (1 - \rho_j^\infty) \frac{\Lambda_{\text{som,max}}}{\Lambda_{\text{som,max}} - \Lambda_{\text{som}}^\infty}, \\ c_{\alpha_{-,j}} &= v_0 \frac{\Lambda_{j,\text{max}}}{\Lambda_j^\infty}, & c_{\beta_{+,j}} &= v_0 (1 - \rho_j^\infty) \frac{\Lambda_{j,\text{max}}}{\Lambda_{j,\text{max}} - \Lambda_j^\infty}. \end{aligned}$$

The interesting question of stability of these states will be treated in future work.

5. FINITE VOLUME SCHEME AND SCALING

5.1. Finite volume scheme. We now present a computational scheme for the numerical solution of model (2.1)–(2.5). The scheme relies on a spatial finite volume discretization of the conservation law (2.2) and adapted implicit-explicit time stepping schemes. Starting point for the construction of a discretization is the transformed equation (3.12). First, we introduce an equidistant grid

$$0 = x_{-1/2} < x_{1/2} < \dots < x_{n_e-1/2} < x_{n_e+1/2} = 1$$

of the interval $(0, 1)$ and define control volumes $I_k := (x_{k-1/2}, x_{k+1/2})$, $k = 0, \dots, n_e$. The mesh parameter is $h = x_{k+1/2} - x_{k-1/2} = (n_e + 1)^{-1}$. The cell averages of the approximate (transformed) solution are denoted by

$$\bar{f}_{\pm,j}^k(t) := \frac{1}{h} \int_{I_k} \bar{f}_{\pm,j}(t, y) \, dy, \quad k = 0, \dots, n_e.$$

To shorten the notation we omit the vesicle index $j \in \{1, 2\}$ in the following. Integrating (2.2) over an arbitrary control volume I_k , $k = 0, \dots, n_e$, and taking into account the transformation formulas (3.11) yields

$$\begin{aligned} 0 &= \int_{I_k} \left[\partial_t f_+ + \partial_y \left(-\frac{D_T}{L(t)^2} \partial_y f_+ + \frac{1}{L(t)} ((v_0(1-\rho) - L'(t)y) f_+) \right) \right. \\ &\quad \left. + \frac{L'(t)}{L(t)} f_+ - \lambda(f_- - f_+) \right] dy \\ &= h \partial_t \bar{f}_+^k + \left[-\frac{D_T}{L(t)^2} \partial_y f_+ + \frac{1}{L(t)} ((v_0(1-\rho) - L'(t)y) f_+) \right]_{x_{k-1/2}}^{x_{k+1/2}} \\ &\quad + h \frac{L'(t)}{L(t)} \bar{f}_+^k - h \lambda(\bar{f}_-^k - \bar{f}_+^k). \end{aligned}$$

We denote the convective flux by $\mathbf{v}_+(t, y) := v_0(1-\rho) - L'(t)y$ and use a Lax-Friedrichs approximation at the endpoints of the control volume

$$(\mathbf{v}_+ f_+)(t, x_{k+1/2}) \approx F_+^{k+1/2}(t) := \left\{ \left(\bar{\beta}_+ \bar{f}_+ \right)(t, x_{k+1/2}) \right\} - \frac{1}{2} \llbracket \bar{f}_+(t, x_{k+1/2}) \rrbracket,$$

with $\{\cdot\}$ and $\llbracket \cdot \rrbracket$ denoting the usual average and jump operators. For the diffusive fluxes we use an approximation by central differences

$$\partial_y f_+(t, x_{k+1/2}) \approx \frac{\bar{f}_+^{k+1}(t) - \bar{f}_+^k(t)}{h}.$$

For the inner intervals I_k with $k \in \{1, \dots, n_e - 1\}$ this gives the equations

$$\begin{aligned} \partial_t \bar{f}_+^k + \frac{D_T}{(hL)^2} (-\bar{f}_+^{k-1} + 2\bar{f}_+^k - \bar{f}_+^{k+1}) &= \frac{1}{hL} \left(F_+^{k-1/2} - F_+^{k+1/2} \right) \\ &\quad + \lambda(\bar{f}_-^k - \bar{f}_+^k) - \frac{L'}{L} \bar{f}_+^k, \end{aligned} \tag{5.1a}$$

while for $k = 0$ and $k = n_e$ we insert the boundary conditions (2.3) to obtain

$$\begin{aligned} \partial_t \bar{f}_+^0 + \frac{D_T}{(hL)^2} (\bar{f}_+^0 - \bar{f}_+^1) &= \frac{1}{hL} \left(\alpha_+ (\Lambda_{\text{som}}) g_+ (\bar{f}_+^0, \bar{f}_-^0) - F_+^{1/2} \right) \\ &\quad + \lambda (\bar{f}_-^0 - \bar{f}_+^0) - \frac{L'}{L} \bar{f}_+^0, \end{aligned} \quad (5.1b)$$

$$\begin{aligned} \partial_t \bar{f}_+^{n_e} + \frac{D_T}{(hL)^2} (\bar{f}_+^{n_e} - \bar{f}_+^{n_e-1}) &= \frac{1}{hL} \left(F_+^{n_e-1/2} - \beta_+ (\Lambda) \bar{f}_+^{n_e} \right) \\ &\quad + \lambda (\bar{f}_-^{n_e} - \bar{f}_+^{n_e}) - \frac{L'}{L} \bar{f}_+^{n_e}, \end{aligned} \quad (5.1c)$$

almost everywhere in $(0, T)$. In the same way we deduce a semi-discrete system for \bar{f}_\pm^k , $k = 0, \dots, n_e$, taking into account the corresponding boundary conditions from (2.3).

To treat the time-dependency we use an implicit-explicit time-stepping scheme. We introduce a time grid $t_n = \tau n$, for $n = 0, \dots, n_t$, and for some time-dependent function $g: [0, T] \rightarrow X$ we use the notation $g(t_n) =: g^{(n)}$. To deduce a fully-discrete scheme we replace the time derivatives in (5.1) by a difference quotient $\partial_t \bar{f}_\pm(t_{n+1}) = \tau^{-1} (\bar{f}_\pm^{(n+1)} - \bar{f}_\pm^{(n)})$ and evaluate the remaining terms related to diffusion in the successive time-point t_{n+1} and all convection and reaction related terms in the current time point t_n . This yields a system of linear equations of the form

$$\left(M + \tau \frac{D_T}{L^{(n)}} A \right) \bar{f}_\pm^{(n+1)} = M \bar{f}_\pm^{(n)} + \tau \bar{b}_\pm^{(n)} + \tau \bar{c}_\pm^{(n)}, \quad (5.2)$$

with vector of unknowns $\bar{f}_\pm^{(n)} = (f_\pm^{0,(n)}, \dots, f_\pm^{n_e,(n)})^\top$, mass matrix M , diffusion matrix A , a vector $\bar{b}_\pm^{(n)}$ summarizing the convection related terms and another vector for the reaction related terms $\bar{c}_\pm^{(n)}$. In the same way we deduce equations for the discretized ordinary differential equations (2.5) and (2.4) which correspond to a standard backward Euler discretization:

$$\begin{aligned} \Lambda_{\text{som}}^{(n+1)} &= \Lambda_{\text{som}}^{(n)} + \tau \sum_{j=1,2} \left(\beta_{-,j} \bar{f}_{j,-}^{0,(n+1)} - \alpha_{+,j} (\Lambda_{\text{som}}^{(n+1)}) g_+ (\bar{f}_{+,j}^{0,(n+1)}, \bar{f}_{-,j}^{0,(n+1)}) \right) \\ &\quad + \tau \gamma_{\text{prod}}^{(n)}, \end{aligned} \quad (5.3)$$

$$\Lambda_j^{(n+1)} = \Lambda_j^{(n)} + \tau \beta_{+,j} (\Lambda_j^{(n+1)}) \bar{f}_{+,j}^{n_e,(n+1)} \quad (5.4)$$

$$- \tau \alpha_{-,j} (\Lambda_j^{(n+1)}) g_{-,j} (\bar{f}_{+,j}^{n_e,(n+1)}, \bar{f}_{-,j}^{n_e,(n+1)}) - \tau c_j h_j (\Lambda_j^{(n)}, L_j^{(n)}), \quad (5.5)$$

$$L_j^{(n+1)} = L_j^{(n)} + \tau h_j (\Lambda_j^{(n+1)}, L_j^{(n+1)}), \quad j = 1, 2. \quad (5.6)$$

Equations (5.2)–(5.6) even decouple. One after the other, we can compute

$$\mathbf{f}^0, L_j^0, \Lambda_k^0 \rightarrow \bar{f}_{\pm,j}^{(1)} \rightarrow \Lambda_k^{(1)} \rightarrow L_j^{(1)} \rightarrow \bar{f}_{\pm,j}^{(2)} \rightarrow \Lambda_k^{(2)} \rightarrow L_j^{(2)} \rightarrow \dots$$

for $k \in \{1, 2, \text{som}\}$ and $j \in \{1, 2\}$.

5.2. Non-dimensionalisation of the model. To transform the model to a dimensionless form we introduce a typical time scale \tilde{t} , a typical length \tilde{L} , etc., and dimensionless quantities \bar{t} , \bar{L} such that $t = \tilde{t}\bar{t}$, $L = \tilde{L}\bar{L}$. Realistic typical values are taken from [13] (see also [19, 23, 21]) which yield the following choices: The *typical length* is $\tilde{L} = 50 \mu\text{m}$, the *typical time* is $\tilde{t} = 100 \text{ s}$, the *diffusion constant* is $D_T = 10^{-1} \frac{\mu\text{m}^2}{\text{s}}$, the *velocity* is $\tilde{v}_0 = 1 \frac{\mu\text{m}}{\text{s}}$. For the *reaction rate* we assume $\tilde{\lambda} = \frac{1}{\text{s}}$. The *typical influx and outflow velocity* is $\tilde{\alpha} = \tilde{\beta} = 10^{-1} \frac{\mu\text{m}}{\text{s}}$. Finally we choose a typical production of $\tilde{\gamma} = 10$ vesicles/sec.

The remaining quantities to be determined are the maximal density of vesicles inside the neurites, the factor which translates a given number of vesicles with length change of the neurite and the maximal capacity of soma and growth cones.

Maximal density. We assume the neurite to be tube-shaped, pick a circular cross-section at an arbitrary point and calculate the maximal number of circles having the diameter of the vesicles that fit the circle whose diameter is that of the neurite. In this situation, hexagonal packing of the smaller circles is optimal, which allows to cover about 90% of the area (neglecting boundary effects). As the *typical diameter* of one vesicle is 130 nm and the neurite diameter is 1 μm , we obtain the condition

$$\underbrace{0.9 \cdot n_{\max} \pi \left(\frac{130 \text{ nm}}{2} \right)^2}_{\text{area covered by } n_{\max} \text{ circles of vesicle diameter}} \leq \underbrace{\pi \left(\frac{1000 \text{ nm}}{2} \right)^2}_{\text{area of neurite cross-section}},$$

which implies $n_{\max} \leq 65$. Now for a tube segment of length 1 μm , one can stack 7 fully packed cross-section slices, each of which has the diameter of the vesicles, i.e., 130 nm. This results in a maximal density of $455 \frac{\text{vesicles}}{\mu\text{m}}$. As the neurite also contains microtubules and as an optimal packing is biologically unrealistic, we take one third of this value as maximal density, which yields $\rho_{\max} = 155 \frac{\text{vesicles}}{\mu\text{m}}$. The *typical density* of anterograde and retrograde particles is fixed to $\tilde{f} := \tilde{f}_+ = \tilde{f}_- = 39 \frac{\text{vesicles}}{\mu\text{m}}$, so that their sum corresponds to a half filled neurite. Thus, for the scaled variables \bar{f}_+ , \bar{f}_- , their sum being $\bar{\rho} = \bar{f}_+ + \bar{f}_- = 2$ corresponds to a completely filled neuron. This implies that the term $1 - \rho$ has to be replaced by $1 - \frac{\bar{\rho}}{2}$.

Vesicles and growth. We again consider the neurite as a cylinder with a diameter of 1 μm . Thus the surface area of a segment of length 1 μm is $A_{\text{surf}} = 2\pi \frac{1 \mu\text{m}}{2} 1 \mu\text{m} \approx 3.14 (\mu\text{m})^2$. We consider vesicles of 130 nm diameter, which thus possess a surface area of $0.053 (\mu\text{m})^2$. Thus the number of vesicles needed for an extension of 1 μm is

$$\frac{3.14 \mu\text{m}^2}{0.053 \mu\text{m}^2} \approx 59, \quad \text{i.e., we fix } c_1 = c_2 = c_h := \frac{58.4 \text{ vesicles}}{\mu\text{m}}.$$

Maximal capacities and minimal values. Finally, we fix the maximal amount of vesicles in the pools and soma to $\Lambda_{\text{som,max}} = 6000$ vesicles and $\Lambda_{j,\text{max}} = 100$ vesicles, and choose the typical values $\tilde{\Lambda}_{\text{som}}$ and $\tilde{\Lambda}_{\text{cone}}$ as half of the maximum, respectively. It remains to fix the minimal length of each neurite as well as the number of vesicles in the growth cone which defines the switching point between growth and shrinkage. We choose a minimal length of 5 μm while the sign of h_j changes when the number of vesicles in the growth cone reaches a value of 50 vesicles. This yields the dimensionless quantities $\tilde{\Lambda}_{\text{min}} = 1$, $\tilde{L}_{\text{min}} = 0.1$. Applying the scaling, model (2.1)–(2.5) transforms to

$$\begin{aligned} \partial_t \bar{f}_{+,j} + \partial_x \left(\kappa_v \bar{f}_{+,j} \left(1 - \frac{\bar{\rho}_j}{2} \right) - \kappa_D \partial_x \bar{f}_{+,j} \right) &= \kappa_\lambda \bar{\lambda} (\bar{f}_{-,j} - \bar{f}_{+,j}), \\ \partial_t \bar{f}_{-,j} - \partial_x \left(\kappa_v \bar{f}_{-,j} \left(1 - \frac{\bar{\rho}_j}{2} \right) - \kappa_D \partial_x \bar{f}_{-,j} \right) &= \kappa_\lambda \bar{\lambda} (\bar{f}_{+,j} - \bar{f}_{-,j}), \end{aligned}$$

in $(0, T) \times (0, \tilde{L}_j(t))$, with dimensionless parameters $\kappa_v = \frac{v_0 \tilde{t}}{L}$, $\kappa_D = D_T \frac{\tilde{t}}{L^2}$, $\kappa_\lambda = \tilde{t} \tilde{\lambda}$, and with boundary conditions (keeping the choices (4.5), (4.8), (4.9))

$$\begin{aligned} \bar{J}_{+,j}(t, 0) &= \kappa_{\alpha+,j} \frac{\tilde{\Lambda}_{\text{som}}(t)}{2} \bar{f}_{+,j}(\tilde{t}, 0) \left(1 - \frac{\bar{\rho}_j(t, 0)}{2} \right), \\ -\bar{J}_{-,j}(t, 0) &= \kappa_{\beta-,j} \left(1 - \frac{\tilde{\Lambda}_{\text{som}}(t)}{2} \right) \bar{f}_{-,j}(t, 0), \\ \bar{J}_{+,j}(t, L_j(t)) &= \kappa_{\beta+,j} \left(1 - \frac{\tilde{\Lambda}_j(t)}{2} \right) \bar{f}_{+,j}(\tilde{t}, \tilde{L}_j(\tilde{t})), \\ -\bar{J}_{-,j}(t, L_j(t)) &= \kappa_{\alpha-,j} \frac{\tilde{\Lambda}_j(t)}{2} \bar{f}_{-,j}(\tilde{t}, 0) \left(1 - \frac{\bar{\rho}_j(t, 0)}{2} \right), \end{aligned}$$

with $\kappa_{\alpha+,j} = \frac{\tilde{t}}{L} c_{\alpha+,j}$, $\kappa_{\alpha-,j} = \frac{\tilde{t}}{L} c_{\alpha-,j}$, $\kappa_{\beta+,j} = \frac{\tilde{t}}{L} c_{\beta+,j}$, $\kappa_{\beta-,j} = \frac{\tilde{t}}{L} c_{\beta-,j}$. It remains to fix the values of the constants appearing in the functions $\alpha_{\pm,j}$, $\beta_{\pm,j}$. As they correspond to velocities, we fix them to the typical in-/outflux velocity

$$\tilde{c} := c_{\alpha+,j} = c_{\alpha-,j} = c_{\beta+,j} = c_{\beta-,j} = 0.1 \frac{\mu\text{m}}{\text{s}}.$$

For the soma and the growth cones we choose half of the maximal amount of vesicles as typical values, i.e., $\bar{\Lambda}_{\text{som}} = 3000$ vesicles, $\bar{\Lambda}_j = 50$ vesicles, $j = 1, 2$. We obtain

$$\begin{aligned}\bar{\Lambda}'_{\text{som}}(t) &= \kappa_{\text{som}} \sum_{j=1,2} \left[\left(1 - \frac{\bar{\Lambda}_{\text{som}}(t)}{2} \right) \bar{f}_{-,j}(t, 0) - \frac{\bar{\Lambda}_{\text{som}}(t)}{2} \bar{f}_{+,j}(\bar{t}, 0) \left(1 - \frac{\bar{\rho}_j(t, 0)}{2} \right) \right] \\ &\quad + \kappa_{\gamma} \tilde{\gamma}_{\text{prod}}(t), \\ \bar{\Lambda}'_j(t) &= \kappa_{\text{cone}} \left[\left(1 - \frac{\bar{\Lambda}_j(t)}{2} \right) \bar{f}_{+,j}(\bar{t}, \bar{L}_j(\bar{t})) - \frac{\bar{\Lambda}_j(t)}{2} \bar{f}_{-,j}(\bar{t}, 0) \left(1 - \frac{\bar{\rho}_j(t, 0)}{2} \right) \right] \\ &\quad - \kappa_h \bar{h}_j(\bar{\Lambda}_j(t), \bar{L}_j(t)),\end{aligned}$$

with $\kappa_{\text{som}} = \frac{\tilde{t}}{\bar{\Lambda}_{\text{som}}} \tilde{c} \tilde{f}$, $\kappa_{\gamma} = \tilde{\gamma} \frac{\tilde{t}}{\bar{\Lambda}_{\text{som}}}$, $\kappa_{\text{cone}} = \frac{\tilde{t}}{\bar{\Lambda}_{\text{cone}}} \tilde{c} \tilde{f}$, $\kappa_h = \frac{\tilde{t}}{\bar{\Lambda}_{\text{cone}}} \tilde{h} c_h$. Finally, for the scaled production function \bar{h} in (2.4) we make the choice $\bar{h}_j = \text{atan}(\bar{\Lambda} - \bar{\Lambda}_{\text{min}}) H(\bar{L} - \bar{L}_{\text{min}})$, $j = 1, 2$, where H is a smoothed Heaviside function. We have

$$\bar{L}'_j(t) = \kappa_L \bar{h}_j(\bar{\Lambda}_j(t), \bar{L}_j(t)), \quad \text{with } \kappa_L = \frac{\tilde{t}}{\bar{L}} \tilde{h}.$$

6. NUMERICAL STUDIES

We present two examples that demonstrate the capability of our model to reproduce observations in biological systems. Both start with an initial length difference of the two neurites. The first example shows that the shorter neurite can become the longer one due to a local advantage of the number of vesicles present in the growth cone while the second showcases oscillatory behaviour in neurite lengths that is observed experimentally. Both simulations are performed in MATLAB, using the finite volume scheme introduced in Section 5.1, using the parameters $\eta = 10$, $n_e = 100$, $\tau = 1e - 4$. We chose $T = 1000$ (corresponding to 27.8 hours) as a maximal time of the simulation, yet when a stationary state is reached before (measured by the criterium $\|f_{\pm,j}^{(n+1)} - f_{\pm,j}^{(n)}\|_2 \leq 1e - 9$), the simulation is terminated. We also set $\lambda = 0$ in all simulations.

6.1. Fast growth by local effects. The first example shows that an initial length deficiency of a neurite can be overcome by a local advantage of vesicles on the growth cone. In this set-up we fixed (all scaled quantities) the following initial data: $L_1^0 = 1.1$, $L_2^0 = 1.0$, $\Lambda_{\text{soma}}^0 = 1$, $\Lambda_1^0 = 0.25$, $\Lambda_2^0 = 1.5$, $\mathbf{f}_1^0 = \mathbf{f}_2^0 = (0.1, 0.1)$. Furthermore, the functions

$$\begin{aligned}g_{\pm}(f_+, f_-) &= 1 - \frac{1}{2}(f_+ + f_-), \quad \alpha_+(\Lambda) = 0.05 \frac{\Lambda}{2}, \quad \alpha_-(\Lambda) = 0.1 \left(1 - \frac{\Lambda}{2} \right) \frac{\Lambda}{2}, \\ \beta_{\pm}(\Lambda) &= 0.7 \left(1 - \frac{\Lambda}{2} \right), \quad h(\Lambda, L) = \frac{\tan^{-1}(\Lambda - \Lambda_{\text{min}})}{1 + \exp(-4(L - L_{\text{min}} - 0.2))}, \quad v_0 = 0.1\end{aligned}$$

were chosen in this example. Figure 3 shows snapshots of the simulation at different times while Figure 4a shows the evolution of neurite lengths and vesicle concentrations over time. The results demonstrate that the local advantage of a higher vesicle concentration in the growth cone of the shorter neurite is sufficient to outgrow the competing neurite. Yet, this requires a weak coupling in the sense that the outflow rate at the soma is small, see the constant 0.05 in α_+ . Increasing this value, the local effect does not prevail and indeed, the longer neurite will always stay longer while both neurites grow at a similar rate as shown in Figure 4b. Thus we consider this result as biologically not very realistic, in particular as it cannot reproduce cycles of extension and retraction that are observed in experiments.

6.2. Oscillatory behaviour due to coupling of soma outflow rates to density of retrograde vesicles. In order to overcome the purely local nature of the effect in the previous example, it seems reasonable to include effects that couple the behaviour at the growth cones to that of the soma via the concentrations of vesicles in the neurites. We propose the following two mechanisms: First, we assume that a strongly growing neurite is less likely to emit a large number of retrograde vesicles as it wants to use all vesicles for the growth process. In addition, we assume that the soma aims to reinforce strong growth and is doing so by measuring

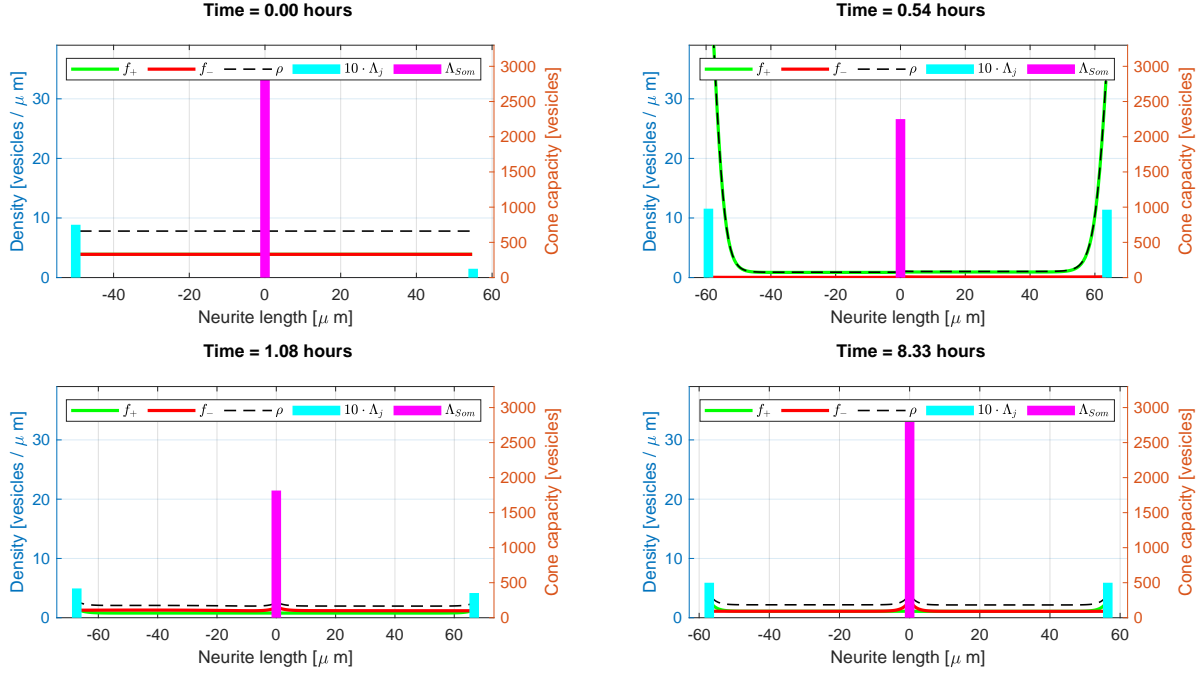


FIGURE 3. The vesicle densities $f_{\pm,j}$, $j = 1, 2$, and pool capacities Λ_k , $k \in \{\text{som}, 1, 2\}$, for the example from Section 6.1 plotted at different time points.

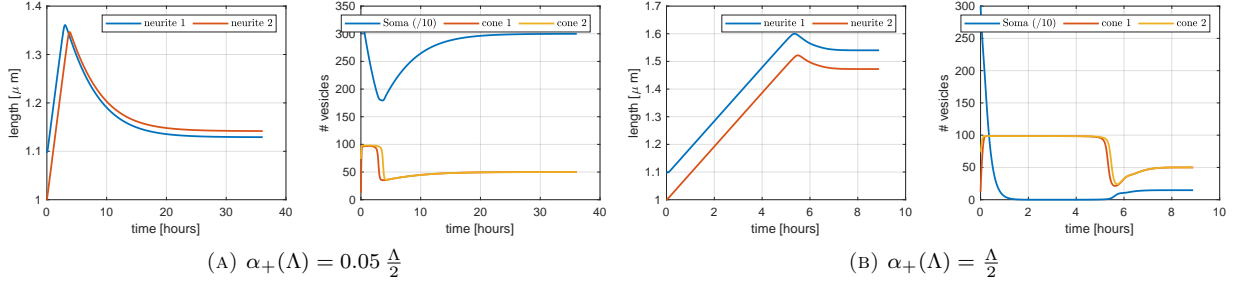


FIGURE 4. The neurite lengths L_j , $j = 1, 2$, and pool capacities Λ_k , $k \in \{\text{som}, 1, 2\}$, for the example from Section 6.1 plotted over time.

the density of arriving retrograde vesicles. The lower it becomes, the more anterograde vesicles are released. Such behaviour can easily be incorporated in our model by choosing

$$g_+(f_+, f_-) = \left(\sqrt{\max(0, 1 - 3f_-)^2 + 0.1} + 0.5 \right) \left(1 - \frac{1}{2}(f_+ + f_-) \right),$$

$$\alpha_+(\Lambda) = 0.6 \frac{\Lambda}{2}, \quad \alpha_-(\Lambda) = \left(1 - \frac{\Lambda}{2} \right) \frac{\Lambda}{2}, \quad v_0 = 0.04.$$

The remaining functions are defined as in Section 6.1. The initial data in this example are $L_1^0 = 1.1$, $L_2^0 = 1$, $\Lambda_{\text{som}}^0 = 1$, $\Lambda_1^0 = \Lambda_2^0 = 0.9$, $f_{\pm,1}^0 = f_{\pm,2}^0 = 0$.

The results are presented in Figures 5 (snapshots) and 6 and are rather interesting: First, it is again demonstrated that the shorter neurite may outgrow the larger one. Furthermore, as a consequence of the non-local coupling mechanism, the model is able to reproduce the oscillatory cycles of retraction and growing

usually observed. Finally, at its stationary state, the model predict one neurite being substantially longer than the other which one might interpret as axon and dendrite.

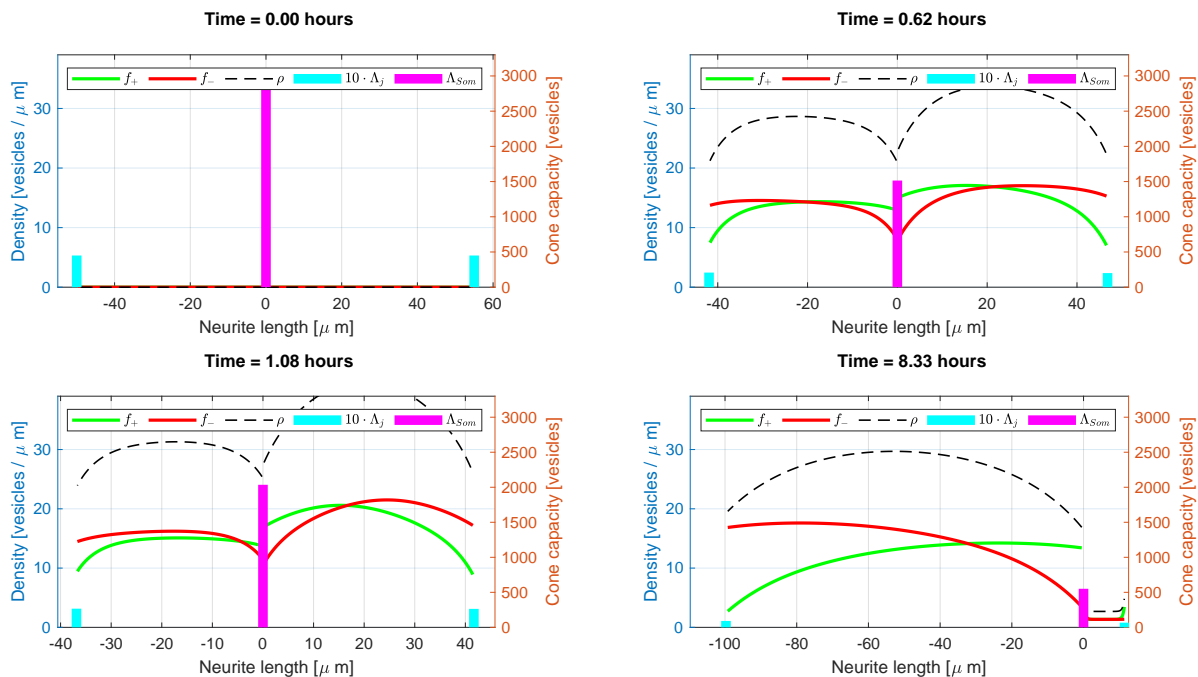


FIGURE 5. The vesicle densities $f_{\pm,j}$, $j = 1, 2$, and pool capacities Λ_k , $k \in \{\text{som}, 1, 2\}$, for the example from Section 6.2 plotted at different time points.

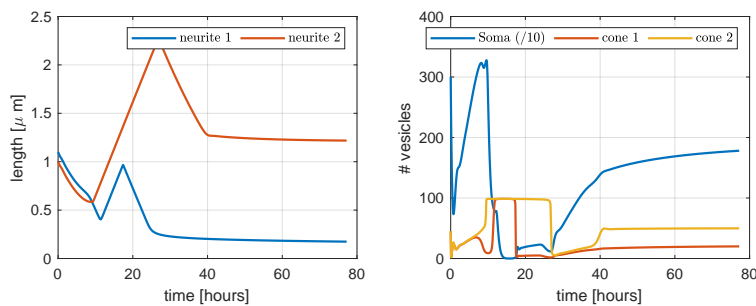


FIGURE 6. The neurite lengths L_j , $j = 1, 2$, and pool capacities Λ_k , $k \in \{\text{soma}, 1, 2\}$, for the example from Section 6.2 plotted over time.

7. CONCLUSION & OUTLOOK

We have introduced a free boundary model for the dynamics of developing neurons based on a coupled system of partial- and ordinary differential equations. We provided an existence and uniqueness result for weak solutions and also presented a finite volume scheme in order to simulate the model. The in silico experiments we perform demonstrate the capability of the model to produce important effect observed in real experiments, based on a conjectured coupling mechanism between growth cones and soma.

A natural question that arises at this point is what can be learned from these results. We think that while the transport mechanisms within the neurites as well as the growth and shrinkage are reasonable and fixed, most of the behaviour of the model is encoded in the coupling conditions. These, on the other hand, allow

for a large variety of choice out of which it will be difficult to decide which is the one actually implemented in a real cell. Furthermore, as the model is focused on transport, many other effects (e.g. due to protein regulation) are neglected. Thus, as a next step for future work, we propose to consider these coupling as unknown parameters that need to be learned using experimental data that comes from experiments. We are confident that this will allow to identify possible interactions between soma and growth cones and will give new insight into the actual mechanisms at work.

ACKNOWLEDGMENTS

GM acknowledges the support of DFG via grant MA 10100/1-1 project number 496629752, JFP via grant HE 6077/16-1 (eBer-22-57443). GM is member of the group GNAMPA of INdAM. We thank Andreas Püschel (WWU Münster) for valuable discussions on the biological background.

REFERENCES

- [1] R. ADAMS, *Sobolev Spaces*, Academic Press, New York-London, 1975.
- [2] S. BRENNER AND L. SCOTT, *The mathematical theory of finite element methods*, vol. 15 of Texts in Applied Mathematics, Springer, New York, third ed., 2008.
- [3] P. BRESSLOFF AND B. KARAMECHED, *Model of reversible vesicular transport with exclusion*, J. Phys. A, 49 (2016), 345602, p. 345602.
- [4] P. BRESSLOFF AND E. LEVIEN, *Synaptic democracy and vesicular transport in axons*, Phys. Rev. Lett., 114 (2015), p. 168101.
- [5] M. BRUNA, M. BURGER, J.-F. PIETSCHMANN, AND M.-T. WOLFRAM, *Active crowds*, in Active Particles, Volume 3: Advances in Theory, Models, and Applications, N. Bellomo, J. A. Carrillo, and E. Tadmor, eds., Springer International Publishing, Cham, 2022, pp. 35–73.
- [6] M. BURGER, M. DI FRANCESCO, J.-F. PIETSCHMANN, AND B. SCHLAKE, *Nonlinear cross-diffusion with size exclusion*, SIAM J. Math. Anal., 42 (2010), pp. 2842–2871.
- [7] J. COOPER, *Cell biology in neuroscience: mechanisms of cell migration in the nervous system*, J. Cell Biol., 202 (2013), pp. 725–734.
- [8] K. DEIMLING, *Ordinary Differential Equations in Banach Spaces*, Springer-Verlag, 1977.
- [9] H. EGGER, J.-F. PIETSCHMANN, AND M. SCHLOTTBOM, *Identification of chemotaxis models with volume filling*, SIAM J. Appl. Math., 75 (2015), pp. 275–288.
- [10] S. ENCALADA, L. SZPANKOWSKI, C.-H. XIA, AND L. GOLDSTEIN, *Stable kinesin and dynein assemblies drive the axonal transport of mammalian prion protein vesicles*, Cell, 144 (2011), pp. 551–565.
- [11] L. EVANS, *Partial Differential Equations*, vol. 19 of Graduate Studies in Mathematics, American Mathematical Society, 2010.
- [12] Y. HATANAKA AND K. YAMAUCHI, *Excitatory Cortical Neurons with Multipolar Shape Establish Neuronal Polarity by Forming a Tangentially Oriented Axon in the Intermediate Zone*, Cerebral Cortex, 23 (2012), pp. 105–113.
- [13] I. HUMPERT, D. DI MEO, A. PÜSCHEL, AND J.-F. PIETSCHMANN, *On the role of vesicle transport in neurite growth: Modeling and experiments*, Math. Biosci., 338 (2021).
- [14] M. KOURBANE-HOUSSENE, C. ERIGNOUX, T. BODINEAU, AND J. TAILLEUR, *Exact hydrodynamic description of active lattice gases*, Phys. Rev. Lett., 120, 268003 (2018).
- [15] G. LIEBERMAN, *Second order parabolic differential equations*, World Scientific Publishing Co., Inc., River Edge, NJ, 1996.
- [16] G. MARINO, J.-F. PIETSCHMANN, AND A. PICHLER, *Uncertainty analysis for drift-diffusion equations*. <https://arxiv.org/abs/2105.06334>.
- [17] H. OLIVERI AND A. GORIELY, *Mathematical models of neuronal growth*, Biomechanics and Modeling in Mechanobiology, 21 (2022), pp. 89–118.
- [18] K. PFENNINGER, L. LAURINO, D. PERETTI, X. WANG, S. ROSSO, G. MORFINI, A. CACERES, AND S. QUIROGA, *Regulation of membrane expansion at the nerve growth cone*, J. Cell Sci., 116 (2003), pp. 1209–1217.
- [19] K. H. PFENNINGER, *Plasma membrane expansion: a neuron's herculean task*, Nat. Rev. Neurosci., 10 (2009), pp. 251–261.
- [20] T. TOJIMA AND H. KAMIGUCHI, *Exocytic and endocytic membrane trafficking in axon development*, Development, Growth & Differentiation, 57 (2015), pp. 291–304.
- [21] K. TSANEVA-ATANASOVA, A. BURGO, T. GALLI, AND D. HOLCMAN, *Quantifying neurite growth mediated by interactions among secretory vesicles, microtubules, and actin networks*, Biophysical Journal, 96 (2009), pp. 840–857.
- [22] A. TWELVETREES, S. PERNIGO, A. SANGER, P. GUEDES-DIAS, G. SCHIAVO, R. STEINER, M. DODDING, AND E. HOLZBAUR, *The dynamic localization of cytoplasmic dynein in neurons is driven by kinesin-1*, Neuron, 90 (2016), pp. 1000–1015.
- [23] F. L. URBINA, S. M. GOMEZ, AND S. L. GUPTON, *Spatiotemporal organization of exocytosis emerges during neuronal shape change*, Journal of Cell Biology, 217 (2018), pp. 1113–1128.

(G. Marino) UNIVERSITÄT AUGSBURG, INSTITUT FÜR MATHEMATIK, UNIVERSITÄTSSTRASSE 12A, 86159 AUGSBURG, GERMANY
Email address: `greta.marino@uni-a.de`

(J.-F. Pietschmann) UNIVERSITÄT AUGSBURG, INSTITUT FÜR MATHEMATIK, UNIVERSITÄTSSTRASSE 12A, 86159 AUGSBURG,
GERMANY
Email address: `jan-f.pietschmann@uni-a.de`

(M. Winkler) TECHNISCHE UNIVERSITÄT CHEMNITZ, FAKULTÄT FÜR MATHEMATIK, REICHENHAINER STRASSE 41, 09126 CHEM-
NITZ, GERMANY
Email address: `max.winkler@mathematik.tu-chemnitz.de`